

C.P. No. 471
(18,071)
A.R.C. Technical Report

C.P. No. 471
(18,071)
A.R.C. Technical Report



MINISTRY OF AVIATION

AERONAUTICAL RESEARCH COUNCIL

CURRENT PAPERS

An Investigation of the Flow over
a Half-Wing Model with 60·5 Degree
Leading Edge Sweepback at a High
Subsonic and Supersonic Speeds

by

F. O'Hara and J. B. Scott-Wilson

LONDON: HER MAJESTY'S STATIONERY OFFICE

1960

EIGHT SHILLINGS NET

C.P. No.471

U.D.C. No. 533.691.13.043.2:533.6.011.35/5:533.691.155.11

Report No. Aero 2567

November, 1955

ROYAL AIRCRAFT ESTABLISHMENT

An investigation of the flow over a half-wing model with
60.5 degrees leading edge sweepback, at a high subsonic
and supersonic speeds

by

F. O'Hara
and
J. B. Scott-Wilson

SUMMARY

Pressure measurements and surface oil flow observations have been made in the N.A.E. 3 ft tunnel on a half-wing model with 60.5 degrees leading-edge sweepback, of aspect ratio 2.828, taper ratio 0.333, and section 6 per cent RAE 101, at Mach numbers 0.81, 1.42, 1.61 and 1.82. The results at $M = 0.81$ show characteristics typical of subsonic flow over a swept wing, including leading-edge separation and a part span vortex; a physical picture of this type of flow, based on the results, is suggested. The results at supersonic speeds show a number of essentially transonic characteristics, including wing shocks and shock induced separation; their presence is consistent with the assumption that the flow depends to some extent on conditions normal to the leading-edge. From a limited analysis of the results, the pressure ratio across the shock for separation is in approximate agreement with the value for two dimensional flow determined by Pearcey.

The possibility of reliable assessment of flow characteristics using the oil flow method is confirmed by the close correspondence found between the flow indications from surface oil patterns and from pressure measurements.

LIST OF CONTENTS

	<u>Page</u>
1 Introduction	5
2 Experimental details	5
3 Range of tests	6
4 Presentation of results	6
5 Results obtained at $M = 0.81$	7
6 Results obtained at $M = 1.61$	8
6.1 Pressure records and oil flow observations	8
6.2 Soap solution visualisation	12
7 Results obtained at $M = 1.42$	12
8 Results obtained at $M = 1.82$	13
9 General assessment of results	14
9.1 Subsonic speed	14
9.2 Supersonic speed	15
9.21 General	15
9.22 Flow characteristics in a section normal to the leading edge	17
9.3 Interpretation of oil flow patterns	19
10 Conclusions	20
List of Symbols	21
References	23

LIST OF ILLUSTRATIONS

	<u>Fig.</u>
Details of model	1
Chordwise pressure distributions for wing incidences $\alpha = 0, 2,$ 4 degrees at $M = 0.81$; $Re.No. = 4.43 \times 10^6$	2
Oil flow observations on upper surface for wing incidences $\alpha = 0, 2, 4$ degrees at $M = 0.81$; $Re.No. = 4.43 \times 10^6$	3
Chordwise pressure distributions for wing incidences $\alpha = 6,$ 8 degrees at $M = 0.81$; $Re.No. = 4.43 \times 10^6$	4
Oil flow observations on upper surface for wing incidences $\alpha = 6, 7, 8$ degrees at $M = 0.81$; $Re.No. = 4.43 \times 10^6$	5
Chordwise pressure distributions for wing incidence $\alpha = 10$ degrees at $M = 0.81$, and corresponding isobar diagram for upper surface; $Re.No. = 4.43 \times 10^6$	6
Oil flow observations on upper surface for wing incidences $\alpha = 9, 10$ degrees at $M = 0.81$; $Re.No. = 4.43 \times 10^6$	7

LIST OF ILLUSTRATIONS (Contd)

	<u>Fig.</u>
Chordwise pressure distributions for wing incidences $\alpha = 12, 16$ degrees at $M = 0.81$; Re.No. = 2.21×10^6	8(a)
Chordwise pressure distribution for wing incidence $\alpha = 20$ degrees at $M = 0.81$; Re.No. = 2.21×10^6	8(b)
Oil flow observations on upper surface for wing incidences $\alpha = 12, 16, 20$ degrees at $M = 0.81$; Re.No. = 2.21×10^6	9
Chordwise pressure distributions for wing incidences $\alpha = 0, 2, 4$ degrees at $M = 1.61$; Re.No. = 4.15×10^6	10
Oil flow observations on upper surface for wing incidences $\alpha = 0, 2, 4$ degrees at $M = 1.61$; Re.No. = 4.15×10^6	11
Chordwise pressure distributions for wing incidences $\alpha = 6, 8$ degrees at $M = 1.61$; Re.No. = 4.15×10^6	12
Oil flow observations on upper surface for wing incidences $\alpha = 6, 8$ degrees at $M = 1.61$; Re.No. = 4.15×10^6	13
Chordwise pressure distributions for wing incidence $\alpha = 10$ degrees at $M = 1.61$, and corresponding isobar diagram for upper surface; Re.No. = 4.15×10^6	14
Oil flow observation on upper surface for wing incidence $\alpha = 10$ degrees at $M = 1.61$; Re.No. = 4.15×10^6	15
Chordwise pressure distributions for wing incidences $\alpha = 12, 16, 20$ degrees at $M = 1.61$; Re.No. = 2.07×10^6	16
Oil flow observations on upper surface for wing incidences $\alpha = 12, 16, 20$ degrees at $M = 1.61$; Re.No. = 2.07×10^6	17
Flow observations releasing soap solution from pressure holes on upper surface for wing incidences $\alpha = 2, 6, 8, 10, 12, 16$ degrees at $M = 1.61$; Re.No. = 4.15×10^6 for $\alpha \leq 10$ degrees; Re.No. = 2.07 for $\alpha > 10$ degrees	18
Chordwise pressure distributions for wing incidences $\alpha = 0, 2, 4$ degrees at $M = 1.42$; Re.No. = 4.15×10^6	19
Chordwise pressure distributions for wing incidences $\alpha = 6, 8$ degrees at $M = 1.42$; Re.No. = 4.15×10^6	20
Chordwise pressure distributions for wing incidence $\alpha = 10$ degrees at $M = 1.42$ and corresponding isobar diagram for upper surface; Re.No. = 4.15×10^6	21
Oil flow observations on upper surface for wing incidences $\alpha = 0, 10$ degrees at $M = 1.42$; Re.No. = 4.15×10^6	22
Chordwise pressure distributions for wing incidences $\alpha = 12, 16$ degrees at $M = 1.42$; Re.No. = 2.07×10^6	23(a)

LIST OF ILLUSTRATIONS (Contd)

	<u>Fig.</u>
Chordwise pressure distributions for wing incidences $\alpha = 18$ degrees at $M = 1.42$; Re.No. = 2.07×10^6	23(b)
Chordwise pressure distributions for wing incidences $\alpha = 0, 2, 4$ degrees at $M = 1.82$; Re.No. = 4.15×10^6	24
Chordwise pressure distributions for wing incidences $\alpha = 6, 8$ degrees at $M = 1.82$; Re.No. = 4.15×10^6	25
Chordwise pressure distributions for wing incidence $\alpha = 10$ degrees at $M = 1.82$ and corresponding isobar diagram for upper surface; Re.No. = 4.15×10^6	26
Oil flow observations on upper surface for wing incidences $\alpha = 0, 10$ degrees at $M = 1.82$; Re.No. = 4.15×10^6	27
Chordwise pressure distributions for wing incidences $\alpha = 12, 16, 20$ degrees at $M = 1.82$; Re.No. = 2.07×10^6	28
Sketch of part span vortex flow for a section normal to the leading edge	29
Sketch of flow with leading edge separation and part span vortex	30
Isobar diagrams for upper surface for wing incidences $\alpha = 0, 2, 4$ degrees at $M = 1.61$; Re.No. = 4.15×10^6	31(a)
Isobar diagrams for upper surface for wing incidences $\alpha = 6, 8, 10$ degrees at $M = 1.61$; Re.No. = 4.15×10^6	31(b)
Comparison of section normal to leading edge with streamwise section, 6 per cent thick RAE 101	32
Pressure distributions on upper surface taken normal to the leading edge for three supersonic speeds at wing incidence $\alpha = 10$ degrees	33

1 Introduction

A programme of work was planned in the 3 ft supersonic tunnel at R.A.E., Bedford to investigate control problems at transonic and supersonic speeds. The first model to become available for tests of this kind was a half wing with 60.5 degrees leading-edge sweepback, fitted over the outer half span with an adjustable trailing edge flap control of 25 per cent chord, and equipped for surface pressure measurements. Pressure distributions and flow visualisation tests have been made with this model at high subsonic speed ($M = 0.81$) and at supersonic speeds ($M = 1.42, 1.61, 1.82$) for a number of control settings. Because of its size and a special turntable mounting arrangement, this model cannot be tested in the transonic working section of the 3 ft tunnel (the model was in fact in process of production before the transonic section was planned) and other models are being manufactured for tests throughout the transonic speed range and also at supersonic speeds.

The data presented in this paper are for zero control deflection only. They give some understanding of the flow over the wing; particular points arising and being discussed include leading-edge separation and wing vortices, wing shocks, and shock induced separation. The reader not concerned with full details should note that paras. 5, 6, 7 and 8 contain mainly factual descriptions of the pressure records and flow observations, and that a general assessment of the results is given in para. 9. Some emphasis is placed, in describing the results, on the correlation of inferences about the flow characteristics made from surface oil patterns with those from pressure measurements; this is done with a view to giving general guidance in the interpretation of oil flow pictures, since this frequently has to be done without supporting evidence from pressure measurements.

Results with control deflected, and of other tests including a comparison of the flow with and without a leading edge roughness band, intended to fix transition, and of the effect of the presence of a half body, will be given in later reports. In addition a comparison will be made with the results of tests on a complete model with the same wing, including overall force measurements.

2 Experimental details

The model used in the investigation was a half wing made of mild steel, mounted in the 3 ft tunnel¹ on a turntable fitted in place of a Schlieren window in one of the sidewalls. The wing planform was one of a systematic series with a leading edge sweepback of 60.5 degrees, an aspect ratio of 2.828, taper ratio of 0.333, and a half span of 15 in; the airfoil section in the stream direction was 6 per cent thick RAE 101, and the incidence range provided by the turntable was from -10 degrees to 20 degrees. The flap type control hinged at 0.75c could be deflected to a number of positions in the range ± 15 degrees using bracket setting pieces. There were sixty pressure holes on the upper wing surface, distributed along streamwise chords at four stations over the span, at $y = 0.355s, 0.547s, 0.741s$ and $0.935s$; the pressure tubes were fed out through the centre of the turntable. Throughout the tests with which this report is concerned, there was a roughness band, consisting of carborundum powder (grade 240) in aluminium paint, over the leading 10 per cent of the wing chord; this was done to fix the position of the boundary layer transition to turbulent flow, thus eliminating undesirable laminar boundary layer separations which may occur if transition is free at low Reynolds numbers². Further details of the model and of the positions of the pressure holes are given in Fig.1.

Flow visualisation on the wing surface was obtained with a method using a mixture of oil and titanium oxide smeared over the surface². The technique of using this method in the 3 ft tunnel is now well developed but satisfactory photographs can not be taken while the tunnel is running, and some distortion which occurred during shutdown is apparent in several of the photographic records of the flow; the distortion is particularly marked in early tests with high incidence at supersonic speeds in which it was considered advisable to reduce incidence to zero as well as to decrease the stagnation pressure before shutdown, because of uncertainty about the effect of the passage of the tunnel shock over the model. In later tests, after experience with the model, shutdown was made with incidences up to 10 degrees, but still at reduced stagnation pressure.

Another method of flow observation, particularly suited for showing the presence of regions of separated flow and something of their extent above the surface, was tried out during the tests; this method makes use of soap solution which was released from selected pressure holes by feeding it in through the pressure tubes. The liquid tended to run on the surface with some distinguishing white foam in attached flow, but left the surface as jets and spray in separated regions. An advantage of the method is that a range of incidence can be explored in one run, whereas with oil flow and similar surface treatments the tunnel has to be stopped and the surface prepared again for each incidence.

3 Range of tests

Surface pressure distributions were obtained at Mach numbers of 0.81, 1.42, 1.61 and 1.82, through an incidence range from $\alpha = -10$ to 20 degrees, except at $M = 1.42$ where the positive incidence was limited to 18 degrees because of wing tip vibration. Oil flow observations were made throughout the incidence range at $M = 0.81$ and 1.61 and for $\alpha = 0, 10$ degrees at $M = 1.42$ and 1.82. The Reynolds number of the flow based on the model mean aerodynamic chord was 4.15×10^6 for $\alpha = -10$ to 10 degrees, and 2.07×10^6 for $\alpha = 12$ to 20 degrees at the supersonic speeds; at $M = 0.81$, the Reynolds number was 4.43×10^6 for $\alpha = -10$ to 10 degrees, and 2.21×10^6 for $\alpha = 12$ to 20 degrees. The test Mach numbers quoted represent corrected speeds at the model; the blockage correction applied to the subsonic case was estimated from Ref.3 and was found to be small (less than 0.01 on Mach number).

4 Presentation of results

The pressure distributions are plotted in the form of pressure coefficients C_p , for wing incidences $\alpha = 0, 2, 4$ degrees at $M = 0.81$ in Fig.2; corresponding oil flow observations are given in the adjoining Fig.3. Pressure distributions and oil flow observations are given for the other incidences tested ($\alpha = 6, 8, 10, 12, 16, 20$ degrees) in Figs.4 to 9; the pressure distribution for $\alpha = 10$ degrees is also given in Fig.6 in the form of isobars on the wing planform, and oil flow observations for $\alpha = 7, 9$ degrees are included in Figs. 5 and 7 respectively.

A similar arrangement has been adopted for a presentation of the results for $M = 1.61$, which are given in Figs.10 to 17; in addition in Fig.18 are given a number of photographs showing the flow resulting from the release of soap solution from the three forward holes at the two outboard pressure stations. The pressure distributions for a range of incidence at $M = 1.42$ together with oil flow observations for $\alpha = 0, 10$ degrees are given in Figs.19 to 23(b), and similarly for $M = 1.82$ in Figs.24 to 28.

The chordwise pressure distributions in Fig.2 show that as wing incidence was increased from zero to 4 degrees, a suction region developed in normal subsonic fashion at the leading edge; this is particularly marked at the outer station where there is a pronounced peak value of negative C_p at $\alpha = 4$ degrees. The corresponding oil flow photographs in Fig.3 show a regular pattern of lines at $\alpha = 0$ and 2 degrees, with a tendency for the lines to curve in slightly towards the wing root, and then curve outwards beyond the stream direction; at $\alpha = 2$ degrees, the clearing away of the oil near the tip indicates the existence of a weak tip vortex. At $\alpha = 4$ degrees, the collection of the oil into chordwise strips suggests the presence of an array of minor vortices, starting from near the leading edge over most of the span and dying away towards the 0.75 chord position. Similar vortices are referred to also at higher incidences and a brief discussion of their possible nature is given in para.9.1.

At an incidence of 6 degrees (Fig.4), the suction peak is flatter and broader over the two outer pressure stations, while at 8 degrees, the suction peak has broadened at $y = 0.547s$, and there are no marked suction peaks at the two outer stations; there are however noticeable minor suction peaks in the upper surface pressure distribution for 8 degrees, for example at the 50 per cent chord position on the pressure station at $y = 0.741s$ and at the 80 per cent chord position on the station at $0.935s$. Following Küchemann's analysis of types of flow on swept wings⁴, the flattened parts of the pressure distributions indicate a region of leading edge separation or separation "bubble"; the secondary suction peaks indicate the presence of vortex flow, apparently arising from a "part-span vortex" running diagonally across the wing at the rear of the separation bubble. On this basis, it appears from Fig.4 that at 8 degrees for example, there is a leading edge separation starting inboard of the station at $0.547s$, and of widening chordwise extent over the outer part of the wing span, increasing to about 65 per cent of the chord at the outer station; the low-pressure axis of the vortex appears to cross the $0.547s$ line at about $0.3c$, $0.741s$ at about $0.55c$ and $0.935s$ at about $0.8c$. The relatively high negative C_p value towards the trailing edge at the outer station appears to be due to the suction effect of the vortex and shows that its influence at the trailing edge spreads inboard of this section. Further discussion of the general physical character of this type of flow is given in para.9.1.

The flow visualisation picture for 8 degrees in Fig.5 shows a region near the leading edge over the outer half of the wing where no movement of the oil has occurred; this appears to indicate a region of separated flow extending from inboards of the $0.547s$ station to about $0.60c$ at the outer station, which in fact corresponds closely to the separated region deduced from the form of the pressure distributions. The pattern of the oil flow immediately behind the separated region suggests a type of vortex flow, with a heavily scoured central or axial region, arising presumably from high air velocities, and oil lines in a spiral form indicating rotation about this axis; the vortex region extends from an apex apparently near the leading edge at the $0.345s$ station, crossing the $0.547s$ line between $0.10c$ and $0.70c$, the $0.741s$ line over the rear 70 per cent of the chord, and $0.941s$ over the rear 40 per cent, and this corresponds approximately to the low pressure region attributed to a part span vortex in the pressure distributions. The leading edge separation is not evident in the oil flow picture for 6 degrees but it can be seen at 7 degrees (Fig.5); these pictures show the array of nearly streamwise vortices noted at 4 degrees, but in an enlarged form.

The pressure distributions for 10 degrees in Fig.6 all show flattened suction regions indicating leading edge separation, starting probably inboard of the inner pressure station, extending to about 0.15c at the 0.547s line, to 0.40c at 0.741s and to at least 0.80c at 0.935s. As at 8 degrees, secondary suction peaks, for example at 0.45c at $y = 0.547s$, and at 0.70c at 0.741s are evidence of the existence of a part span vortex, crossing the wing diagonally behind the separated region. The field of influence of the vortex at the trailing edge appears to lie outboard of $y = 0.547s$ at which the upper surface pressure returns to near free stream conditions. The oil flow picture for 10 degrees in Fig.7 is overdeveloped on the inner half of the wing (it is difficult to achieve adequate development simultaneously over the whole surface) so that the vortex pattern is not clearly shown, but the separated region is well defined; the vortex pattern, including the part-span vortex and marked streamwise vortices, is more evident at 9 degrees (Fig.7), but the oil pattern is not fully developed over the outer part of the wing and the extent of the separated region is not accurately defined.

The pressure field on the wing at $\alpha = 10$ degrees is also presented in Fig.6 in the form of an isobar diagram, which has been freely drawn from the measured pressure distributions. The concentration of isobar lines corresponds to the region of pressure recovery in the pressure distribution, and the aft boundary of this concentration appear to mark approximately the limit of influence of the vortex, since the latter makes a major suction contribution to the pressure distribution. The core of the vortex is assumed to be the line along which the vortex has the maximum effect on the pressure distribution, but this will not coincide with the peak suction position if there is a pressure gradient in the basic distribution on which the vortex effect is superimposed; in general, the vortex lies in a pressure recovery region so that the core can be expected to lie slightly aft of the peak suction region.

The pressure distributions (for the upper surface only) at higher incidences in Fig.8(a) and 8(b) show a separation over the whole tip chord station at 12 degrees and it spreads inwards with incidence so that it covers the outer half of the wing at 20 degrees; this is also shown by the oil flow photographs in Fig.9. The considerable spanwise variation of pressure in the separated region is noteworthy; this is discussed further in para. 9.1.

6 Results obtained at $M = 1.61$

6.1 Pressure records and oil flow observations

The pressure records for $M = 1.61$ in Fig.10 show that as the incidence was increased from zero to 2 degrees a definite step developed near 0.82c in the upper surface chordwise pressure distribution at $y = 0.935s$, indicating the existence of a weak compression shock in that region. At $\alpha = 4$ degrees, steps in the pressure distributions are evident at 0.8c at $y = 0.741s$, and at 0.76c at 0.935s, so that the upper surface shock appears to have spread inwards and also moved forward by a small amount. The appearance of a wing shock is an indication that the character of the flow in that region of the wing is transonic, and probably determined approximately by conditions normal to the leading edge, on which theoretically the flow over an infinite

yawed wing alone depends. Following lines of argument similar to those used by Pearcey^{*5} in an analysis of two dimensional transonic flow, certain inferences about the flow can also be made from the nature of the pressure distribution at the trailing edge. The trends at the trailing edge of the pressure coefficient curves for $\alpha = 0$ and 2 degrees in Fig.10 show the trailing edge pressure coefficient to be near the free stream value, but at 4 degrees it appears to be -0.1 approximately at $y = 0.935s$, and a rather lower negative value at $y = 0.741s$; this departure from the free stream conditions at the trailing edge appears, as in two dimensional flow, to be an indication of separation behind the shock^{**}.

The oil flow pictures in Fig.11 show lines of regular pattern at zero incidence, but at 2 degrees there is a noticeable discontinuity in the direction of the oil lines near the 85 per cent chord line over the outer 20 per cent of the wing span. At 4 degrees there is a more definite collection of oil into a line running from near the middle of the control hinge line ($y = 0.75s$) towards the 90 per cent chord line at $y = 0.935s$; this line starts inboard near the position of the shock indicated by the pressure distribution at $0.741s$, but is aft of the shock position at the outer station. The oil lines on the inner part of the control surface run in a nearly spanwise direction, but in the region behind the shock, the lines can be seen to turn and run forward towards the shock; this is an indication of boundary layer separation in accordance with inferences already made from the pressure distributions. The clearing away of the oil in the vicinity of the tip appears to be due to a tip vortex.

The pressure records for 6 and 8 degrees in Fig.12 show steps, some of which are of considerable chordwise extent. To simplify discussion of the results, the position of the step (and shock) is defined by the point at which the pressure gradient is a maximum; this point is generally near the middle of the step. The steps in the pressure distributions for the two outer stations at 6 degrees have moved forward in comparison with 4 degrees being at about $0.64c$ at $0.935s$ and at $0.71c$ at $0.741s$; there also appears to be an indication of a weak shock at about $0.40c$ at $0.547s$. At 8 degrees, the shock position at $0.935s$ has moved forward to $0.52c$, that at $0.741s$ to $0.64c$, while the step at $0.547s$ has moved back to $0.53c$; there is also a small step at $y = 0.355s$ at $0.27c$. The trends of the curves suggest that the trailing edge pressures at the two outer stations at both 6 and 8 degrees are considerably below the free stream value, and this is interpreted, as at 4 degrees, as indicating shock induced separation extending to the trailing edge; at $y = 0.547s$, the trailing edge pressures are not sufficiently definitely indicated for inferences to be made about the flow conditions. The backwards movement of the shock at $0.547s$ with increase of incidence from 6 to 8 degrees is

* A brief outline of some of Pearcey's findings may assist in understanding subsequent interpretations of the pressure records. Pearcey shows that flow separation extending to the trailing edge behind a shock on the upper surface results in the upper and lower surface pressures equalising at the trailing edge at a pressure below the free stream level; he also suggests that the trailing edge pressure tends to diverge from the free stream value when the pressure behind the shock falls below the sonic value, and notes that a marked divergence can occur when supersonic conditions extend to the trailing edge, where the pressures on the two surfaces can then equalise with a supersonic expansion from the lower surface.

** Deviation of the trailing edge pressure from the free stream value on a finite swept wing may also result from a vortex crossing the trailing edge (like the part-span vortex in the subsonic tests) but consideration of this possibility is left till later (see paras. 7 and 9.2).

consistent with Pearcey's findings for attached flow behind the shock; forward movement starts when flow separation behind the shock spreads to the trailing edge.

In the oil flow picture for 6 degrees in Fig.13, the pattern in the vicinity of the shock position is clearly defined, partly because of proximity to the control hinge line; there are however discontinuities in the direction of the oil lines just forward of the hinge line at about $y = 0.75s$, and starting from this region there is a lightly defined cleared line inclined slightly forward of the hinge line, the forward edge of which cuts the $0.935s$ line near $0.65c$. This type of cleared line is seen in a more definite form at 8 degrees, intersecting the $0.741s$ line at $0.65c$ approximately, and (so far as can be seen through the insufficiently developed and distorted pattern) appears to be heading for near the mid-chord position at $0.935s$. The intersections of the cleared line with the pressure stations at both 6 and 8 degrees lie very close to the positions of the steps in the pressure distributions. The physical significance of the cleared line is easier to understand when it is explained that observation during the test run showed that it was a line along which oil collected, and it only became cleared of oil after the incidence was reduced to zero in preparation for shutdown of the tunnel; the line is interpreted in fact as indicating the forward boundary of a region of separated flow beginning at the foot of the shock, at which some of the oil flowing through the shock appears to come to rest. On the flow picture for 8 degrees a faint oblique oil line can be seen starting slightly aft of the cleared line near the inner control bracket, and intersecting the $0.547s$ line at $0.60c$; this is aft of the corresponding step in the pressure record, possibly as a result of oil movement in the shutdown stage. Some explanation of the oil line may be necessary in view of the fact that it has already been noted, in considering the pressure records, that there is no indication at 8 degrees of separation extending to the trailing edge on the inner part of the wing, where the oblique leg of the shock lies; this does not however preclude the possibility of a small closed bubble along the shock leg at which some of the oil collects, and there may in fact be separation regions of variant extent but closing before the trailing edge, and without marked effects on the pressures there. More easily interpreted results were obtained in later tests in which the incidence was maintained at the test setting during shutdown; an oil line then appeared in the oil flow photograph in place of the cleared line, just behind the shock (see, for example $\alpha = 10$ degrees, $M = 1.82$ in Fig.27).

Other points to note in the oil flow pictures for 6 and 8 degrees are the oil lines running forward in the separated region behind the shock, outboard of $y = 0.65s$ and $0.50s$ at $\alpha = 6$ degrees and 8 degrees respectively, and the progressive development of the tip vortex. At 8 degrees there is a region apparently separated outboard of the vortex at the tip; inboard of the main cleared area assumed to indicate the vortex, there is another line starting from the tip, the significance of which is not fully understood, but which could be an indication of a secondary separation of the cross-flow leading to a small bubble on the inside of the tip vortex sheet.

The pressure records for $\alpha = 10$ degrees in Fig.14 show steps in the pressure distributions at about $0.34c$ at $y = 0.935s$, at $0.57c$ at $0.741s$, at $0.54c$ at $0.547s$, and at $0.32c$ at $0.355s$. The shock positions at the two outer stations have moved forward with increase of incidence from 8 to 10 degrees, while at the two inner stations they have moved slightly aft. From the trend of the curves, the trailing edge pressure appears to lie below the free stream value at the two outer stations, indicating separated flow there, and a similar inference can possibly also be made at $0.547s$; the significance of the sudden slight decrease in pressure near the trailing edge on the station at $0.547s$ is not clear. The oil flow picture for 10 degrees in

Fig.15, shows a cleared line of which the forward edge interests $y = 0.935s$ at about $0.35c$, $0.741s$ at $0.60c$, $0.547s$ at $0.60c$, and $0.355s$ at about $0.35c$; these points lie slightly aft of the corresponding pressure steps, and the cleared line is interpreted as at 8 degrees, as the forward boundary of a separated region beginning at the shock. The shape of the shock is shown approximately therefore by the cleared line; it is notable for the curving forward of the outer part in the tip region, and for the inner oblique leg inclined forward to the leading edge, of which there was also an indication at 8 degrees. The way in which the shock pattern develops is discussed in para. 9.2, but it may be noted here that whereas the outer, approximately spanwise and unswept part of the shock is required to effect pressure recovery before the trailing edge, the inboard oblique leg appears to be the result of wall influence, and assists in producing deflection of the flow from a direction inclined towards the normal to the leading edge back to alignment with the wall boundary. The direction of flow in front of the shock is shown in Fig.15 by the oil lines running in a regular manner from the leading edge; they are inclined slightly away from the stream direction towards the normal to the leading edge, along which the main acceleration of the flow occurs.

An isobar diagram derived from the pressure records for $\alpha = 10$ degrees is also given in Fig.14; there is a close correspondence apparent between the shape of the region of concentration of the constant pressure lines and that of the curved shock line in the oil flow record (Fig.15). It has been shown⁶ that conditions are critical in a flow when the local velocity component normal to the isobars becomes sonic; the correlation obtained between the isobar pattern and the shock position shows that the velocity component normal to the isobars is of special significance also in relation to shock waves.

The upper surface pressure distributions at 12, 16 and 20 degrees in Fig.16 were obtained at reduced stagnation pressure. They show less marked pressure steps, and a definite picture of the shock pattern on the wing is not given by the records. The flatness of the pressure distributions at $0.935s$ at $\alpha = 12$ degrees, and at inboard stations at 16 and 20 degrees may indicate separation of the flow from the leading edge; there is some confirmation of this in the oil flow patterns in Fig.17, but more definite evidence is presented later from the soap solution tests (para.8.2). The oil flow records for these higher incidences in Fig.17 are notable however for a vortex type of pattern running obliquely across the wing; the pattern is unfortunately too far inboard for a major effect to be expected in the pressure measurements. This form of pattern has however also been noted at $\alpha = 10$ degrees at $M = 1.42$ and is discussed further in para. 7.

The oil flow pictures for the higher incidences show considerable distortion. There is for example, no definite boundary apparent at $\alpha = 20$ degrees in Fig.17 between the streaming lines from the leading edge and the vortex type pattern, and the boundaries at 12 and 16 degrees are ill-defined; this may be attributed to the fact however that the streaming lines were observed to appear during run-up of the tunnel at zero incidence, and do not necessarily represent accurately conditions at the nominal incidences. There is evident distortion also in the picture for $\alpha = 10$ degrees in Fig.15; the short oil tails behind the oblique leg of the shock and the long tails over the outer part of the wing resulted from the flow of oil which had accumulated along the shock, during the change of conditions at shutdown. Assessment of some of the oil flow pictures may be more difficult if it is not known, from observation, which of the lines formed in the run-up and shutdown stages.

6.2 Soap solution visualisation

The photographs in Fig.18 show the results of releasing soap solution from the three forward holes in the two outboard pressure stations for a range of wing incidence. It can be seen from these pictures, for example for $\alpha = 8$ or 10 degrees that direct evidence of separation, and also an indication of the depth of separation above the wing, are given by the soap solution spray leaving the surface. The shock appears to be shown by a line concentration of the soap solution on the surface and though its position can not be accurately determined because of the photographic viewpoint*, the indications of shock position and separation near the tip appear generally to confirm the inferences already made from the oil flow pictures. At 12 and 16 degrees, where the oil flow pictures were not clear, the soap flow pictures show fluid jets pointing in various directions; at 16 degrees gathering of soap froth on the surface leaves no doubt of separation over the tip.

7 Results obtained at M = 1.42

The pressure records for M = 1.42 in Figs.19 to 23 show many features similar to those for M = 1.61. One of the differences to be noted is that the shock position on the wing for a given incidence is further forward than at the higher Mach number; for example the pressure steps at M = 1.42 for $\alpha = 5$ degrees in Fig.20, are at 0.42c at $y = 0.935s$, at 0.55c at 0.741s, and at 0.25c at 0.547s, compared to 0.64c, 0.71c, and 0.40c respectively for $\alpha = 6$ degrees at M = 1.61, in Fig.12. From the variation of the trailing edge pressures indicated by the trends of the curves towards the trailing edge, the development of the separated flow with incidence appears to take place at comparable rates at both Mach numbers.

Flow visualisation pictures for $\alpha = 0$ and 10 degrees are given in Fig.22. The zero incidence picture shows marked spanwise flow near the tip. At 10 degrees, there is a line along which oil is collected crossing the pressure station at 0.355s at 0.24c, 0.547s at 0.42c and 0.741s at 0.48c; in these tests, the model incidence was maintained during shutdown and the oil line position in the photographs is the same as during the test conditions. The points of intersection of the oil line with the pressure stations lie slightly aft of the corresponding pressure steps and, as at M = 1.61, the line marks the forward boundary of a separated region behind the shock. The oil line therefore provides an approximate indication of the shock position on the wing; it terminates abruptly however outboard of the pressure station at 0.741s, whereas in the isobar diagram in Fig.21, the concentration of isobars, indicating the shock position, continues to near the leading edge at $y = 0.935s$, and it appears that the oil flow pattern at the tip had not been given sufficient time for full development.

The curved form of the shock at 10 degrees is generally similar to that at M = 1.61, with an outer part approximately spanwise in direction but curving forward at the tip, and an inner oblique leg. In the oil flow picture, behind the oblique leg of the shock there is a cleared region near the inner end of the control with neighbouring oil lines in a spiral form, and these characteristics are suggestive of the vortex type pattern already noted in a more marked form in the pictures for 12, 16 and 20 degrees at M = 1.61 in Fig.17. This type of oil pattern also has a family resemblance to that for a part-span vortex in subsonic flow, for example, $\alpha = 8$ degrees at M = 0.61 in Fig.5. A feature of the subsonic flow in the vicinity of the part span vortex is the existence of minor suction peaks in the pressure

*The photographs were of necessity taken through the Schlieren window and the range of view available was in consequence restricted.

distributions; the idea of a vortex type flow crossing the wing obliquely behind the shock at $M = 1.42$ is to some extent supported by the presence of suction "bumps" in the pressure distributions in Fig.21, centred at 0.82c at $y = 0.741s$ and aft of 0.90c at 0.935s. The possible nature of the flow in the region behind the shock is discussed further in para. 9.2.

Another point to note in the oil flow pattern for 10 degrees is the apparent discontinuity in the direction of flow near the root trailing edge, suggesting a shock originating at the juncture of the wing trailing edge and the wall. This type of shock is more highly swept back at higher speeds, and hence unlikely to appear on the surface of the wing; there was no apparent evidence of it at $M = 1.61$.

8 Results obtained at $M = 1.82$

The pressure records for $M = 1.82$ in Figs.24 to 28 show similar features to those for $M = 1.61$ and $M = 1.42$. Generally the steps in the pressure distributions indicating the wing shock position are further aft than at $M = 1.61$, and the shock does not definitely show up on the records until $\alpha = 4$ degrees. The trend in the curves towards the trailing edge suggests that the divergence of the trailing edge pressure associated with shock induced separation occurs at lower incidences than at the lower Mach numbers. The forward movement of the shock with incidence continues up to 10 degrees, but at higher incidences there are less definite indications of shock position, and the flow appears to separate from the leading edge over an increasing part of the span, from the tip inwards.

The oil flow photograph in Fig.27 for zero incidence shows only a small amount of spanwise drift. There is a well defined oil pattern at $\alpha = 10$ degrees, which was obtained by keeping the incidence at the test value during tunnel shutdown. The oil line across the wing intersects the station at 0.355s at 0.42c, 0.547s at 0.72c, 0.741s at 0.69c and 0.935s at about 0.60c; the position of the line therefore corresponds closely to the shock position determined by the pressure steps which are at 0.45c at $y = 0.355s$, 0.70c at $y = 0.547s$, 0.67c at $y = 0.741s$, and 0.60c at 0.935s. This oil flow picture establishes more satisfactorily than those at the lower Mach numbers, the near correlation of the oil line to the shock position on the wing. The shape of the shock line includes as in the previous cases, an outer part inclined forward slightly towards the leading edge in the direction towards the tip, and an oblique leg swept forward towards the leading edge well inboard of $y = 0.355s$. The direction of flow in front of the shock is shown clearly by the regular pattern of lines in a direction inclined towards the normal to the leading edge, and the change of direction of flow through the shock is also evident, particularly on the inner part of the oblique leg of the shock.

There is a suggestion behind the oblique leg of the shock in the oil flow picture, of the vortex type pattern discussed in para. 7, but supporting evidence from the pressure records is lacking because the region most affected crosses only the inner pressure station and the indications in the pressure curve at that station are not conclusive.

There is a marked effect on the oil flow at the inner end of the control, due to leak through the unfilled slot; there is an apparent indication of the effect produced in this region aft of 0.8c in the pressure distribution for $y = 0.547s$ in Fig.26. The effect of the tip vortex is also clearly shown by the oil flow extending to about 10 per cent of the span near the trailing edge; its influence in the pressure distribution is indicated by the suction rise aft of 0.80c on the curve for $y = 0.935s$ in Fig.26. The oil lines running spanwise and forward indicate separated flow behind the shock in the region between the slot and tip effects.

9 General assessment of results

9.1 Subsonic speed

The results obtained at $M = 0.81$ show the features normally expected with increase of incidence for a thin wing of moderately swept leading edge, including leading edge separation and a part span vortex. The development of the flow shown by the pressure and oil flow records in combination, however, suggests a more complete physical picture of the flow than seems previously to have been given for the part span vortex flow on a swept wing^{4,7}.

Evidence has been obtained of separation of the wing boundary layer from the leading edge at moderate incidences; the separation probably begins in fact fairly close to the forward stagnation point. It has also been found that there is a low pressure vortex region at the rear of the separation, and following Küchemann's model for edge vortex sheets on a narrow delta wing⁷, it is suggested that the vortex at the rear of the separation also arises from rolling up of a vortex sheet formed by the separated boundary layer. A sketch of the possible flow layout for a cross section normal to the leading edge is shown in Fig.29. The vortex sheet entrains mainstream air which is drawn down on to the wing surface, forward under the vortex core and into the vortex; on a swept wing there is a spanwise component of velocity and the air drawn into the vortex flows out along the vortex core. There is a streamline meeting the surface at the "dividing point", or "attachment point", which separates flow into the vortex from the flow passing over the rear of the wing. The entrained air flowing forward forms a boundary layer on the surface and, being subject to an adverse pressure gradient after passing under the vortex core, may separate from the surface at a "rear, or secondary, separation point" so that as indicated in Fig.29, a bubble of low energy air remains in the separated region. The general nature of the flow over the wing is envisaged as sketched in Fig.30, for a case of leading edge separation over the outer part of the span; the separation is assumed to result in a free vortex sheet which starts at an apex at the inner point of separation on the leading edge, folds back over on to the wing and effectively rolls up in a conical form over the wing surface. The mainstream air drawn into the vortex flows out along a spiral path on the surface of the vortex sheet. The dividing point and rear separation point of the cross-section of the flow can be seen to lie on lines from the apex along which there is radial flow but no cross flow, and the separation bubble, contained within radiating lines, expands in size with distance along the span.

Viewing the oil flow patterns obtained on the wing in the light of this picture of the flow, the extent of the bubble and the position of the rear separation line are clearly shown for example in Fig.7 for $\alpha = 10$ degrees; the dividing line is less easy to place exactly, but it can be approximately determined as the aft boundary of the oil lines in a curved or spiral form (indicating the vortex motion) which can be more clearly seen in the pictures for $\alpha = 9$ degrees (Fig.7) or $\alpha = 8$ degrees (Fig.5).

In a number of the oil flow photographs (including those for 8 and 9 degrees) the presence near the leading edge has been noted of what appears to be an array of minor vortices. There is no obvious sign of their presence in the pressure distributions but it is probable that their effect is too fine-grained to be detected by the relatively widely spaced pressure points. The oil flow photographs for some incidences and particularly on the outer half of the wing at 6 degrees, give the impression of superimposed vortex patterns, with lines in the form associated with a part span vortex, crossing over the minor vortex patterns. It is possible therefore that the minor vortices occur in an underlayer, but the mechanism by which the superimposed flow is developed is not yet understood.

Attention was drawn in para. 5 to the appreciable spanwise variation of pressure in the separated region over the outer part of the span at higher incidences. In a study of separated flow in two dimensions, Norbury and Crabtree⁵ show that the pressure distribution over an aerofoil with a "long bubble" type of separation can be determined by relating solutions for the purely external flow and for the viscous flow inside the bubble, considered separately; in considering the latter aspect of the problem they show that the pressure conditions inside the bubble depended largely on conditions at the rear of the bubble. Probably something similar applies in three dimensional conditions so that the pressure inside the separated region is affected by the part span vortex, which appears to become less concentrated and produces smaller suction effects for positions further out on the wing span. One would expect that inside the bubble, associated with the pressure variation, there would be spanwise velocity or circulatory flow induced by the part span vortex at the rear, but there is no evidence of this kind of flow in the oil patterns.

9.2 Supersonic speeds

9.21 General

The main feature of the results obtained at supersonic speeds is the development of a shock wave on the wing, extending inwards from the tip region as incidence is increased. A brief outline of the development of the flow and the shocks on the wing itself as deduced from the experimental results for $M = 1.61$ at which both pressure measurements and oil flow observations were made throughout the incidence range, is as follows. At zero incidence, no shock is apparent on the wing, but as incidence is increased to 2 degrees and then 4 degrees, a compression shock, approximately parallel to the trailing edge, forms in the tip region near the trailing edge, and this shock moves forward slightly and extends inwards over about half the span as incidence is increased to 6 degrees. At 6 degrees, the inner part of the shock has started to curve forward slightly and at 8 degrees, a definite oblique leg, inclined forward to the leading edge, has developed, adjoining the approximately spanwise portion of the shock over the outer part of the wing; at 10 degrees the oblique leg of the shock has grown stronger and runs to near the leading edge, while the outer part of the shock has moved forward and also curves forward slightly towards the leading edge in the tip region. Shock induced separation behind the shock extending to the trailing edge is first evident in the tip region at 4 degrees, and by 10 degrees shock induced separation behind the shock has spread over the outer half of the wing.

An impression of the variation with incidence of the pressure pattern on the part of the wing covered by the pressure stations is given by the isobar diagrams in Fig.31 (a and b), which have been freely drawn from the pressure coefficient curves for $\alpha = 0$ to 10 degrees at $M = 1.61$. The shock position on these diagrams is indicated by a band of concentration of the isobar lines, and this can be seen to develop in the tip region near the trailing edge as incidence is increased from zero to 2 and then 4 degrees. The region of intense concentration spreads inwards and curves forward as the incidence is further increased, showing the development of the oblique leg of the shock. The region of shock induced separation is shown also by the constant pressure area behind the shock, and the spreading of this region as incidence is increased, is associated with a forward movement of the isobar concentration in the vicinity of the tip.

The experimental results obtained at $M = 1.42$ and 1.82 are generally similar to those for $M = 1.61$; they show the presence of a shock over the outer part of the wing at low incidence, its extension inwards and the development of an oblique leg on the inboard part of the wing. The outer

part of the shock at $M = 1.42$ is forward of that at $M = 1.61$ for a given incidence and further aft at $M = 1.82$.

These results have certain implications with regard to the general physical nature of the flow, which are now briefly considered; some aspects of the flow are discussed in further detail in the following Section (para. 9.22). The presence of a shock on the wing at supersonic speed suggests that the flow depends on a component, subsonic in value, of the free stream velocity; theoretically the flow over an infinite yawed wing depends only on the velocity normal to the line of sweepback, and it seems probable (noting that conditions normal to the leading edge are subsonic up to $M = 2.0$) that the flow over the finite swept wing can be assessed to some extent in terms of this velocity component. On this basis, the results for $M = 1.61$, for example, suggest that conditions normal to the leading edge at low incidence (< 4 degrees) are supercritical over the outer part of the wing; the shock position on the wing is determined by the pressure recovery required over the aft part of the wing. The spread inwards of the shock with increase in incidence shows the development of supersonic conditions normal to the leading edge. The sweep forward of the inboard end of the shock and the appearance at 8 degrees of an oblique leg adjoining the outer part of the shock are notable in showing the influence of the wall; the position of the oblique leg of the shock apparently depends on the requirement for deflection of the flow from a direction inclined towards the normal to the leading edge (along which acceleration of the flow mainly occurs) back to alignment with the wall boundary.

It is of interest to note that theoretical estimates for swept wings at zero incidence by Neumark⁹ show that it is possible for critical conditions to occur first in the tip region for highly swept wings. Also it appears from theoretical estimates for swept wings by Küchemann¹⁰ that at subcritical Mach numbers, the suction forces on the surface are shifted back and reduced in the root region, and forward and increased in the tip region, in comparison with loading conditions for an unswept wing; this could lead to critical conditions being attained first in the tip region and this is, in fact, the rule for wings like the one considered here; it further suggests the possibility, for supercritical conditions over part of the wing only, of supersonic regions diminishing in extent with distance inboard from the tip; the wing shock could thus be of reduced strength inboards and also further forward.

The relative positions of the shock at different points over the span are affected also by the forward movement associated with the development of shock induced separation behind the shock. The incidence and extent of separation depend on a number of factors, including shock strength, which result in its occurrence first in the vicinity of the tip, so that the outer part of the shock tends to curve forward, as the separation grows there, well in advance of separation on the inner part of the wing. It is also possible that the shock position may be affected by tip effects; the presence of a tip vortex was noted in the oil flow pictures and its influence extended up to about 10 per cent of the wing span near the trailing edge at higher incidences.

The forward movement of the shock associated with separation results in extensive separated regions at high incidences; for $\alpha = 12$ degrees at $M = 1.61$, the flow appears separated over at least the outer 10 per cent of the wing tip, and larger parts of the outer wing are separated at higher incidences. The practical implications of the occurrence of large separated regions at supersonic speeds are similar to those at subsonic speeds. The possibility of inequality in the large loss of lift in the tip regions could lead to wing dropping, and buffeting may be associated with separations; separation over the outboard control can result in loss of control effectiveness. Consideration is being given to the possibility of testing devices to

alleviate or delay separation and its effects, and to the possibility of establishing some correlation for the swept wing between separation and buffeting.

Another feature of the flow, first observed on the oil flow pictures for 12 degrees and over at $M = 1.61$, and also at $\alpha = 10$ degrees at $M = 1.42$ and 1.82 , is the presence of a vortex type pattern behind the oblique leg of the wing shock. The idea of a vortex type flow behind the shock is supported by the presence of suction "bumps" in the pressure distribution for $\alpha = 10$ degrees at $M = 1.42$; there is in fact in this case a similarity to the characteristics of the pressure records and oil flow observations for the subsonic part span vortex. An analogy may be drawn between the closing of a swept leading edge bubble by a vortex in subsonic conditions as described in para. 9.1, and the closing of a swept shock induced separation bubble by a vortex in supersonic conditions. The apparent vorticity in the latter case is however much less marked than in subsonic conditions.

The shock patterns on finite swept wings obtained in previous investigations^{11,12} do not appear to have shown the main wing shock in so well defined a form as in the present tests. This was due in some cases to tests being made at lower Mach numbers (in the vicinity of $M = 1.0$) on wings with less leading edge sweep; in these conditions, other shocks, arising for example at the junction of the wing trailing edge and body, and so on, are more likely to cross the wing surface and complicate the shock pattern, so that the wing shock depending on flow conditions normal to the leading edge is not shown in a straightforward manner.

9.22 Flow characteristics in a section normal to the leading edge

In the previous paragraph, the characteristics of the flow over the wing have been assessed generally in terms of conditions normal to the leading edge. It is not to be expected that an exact correlation should be possible on a finite wing, because of root and tip effects, and also in the present case, because of taper which results in the trailing edge becoming supersonic for a local velocity in the stream direction greater than $M = 1.46$, while the leading remains subsonic up to about $M = 2.0$. It is still of interest however to check how the flow normal to the leading edge compares with two dimensional flow for approximately equivalent conditions; for this purpose the pressure distributions are considered for a section normal to the leading edge and intersecting it at $y = 0.741s$.

It is of course necessary to consider the flow not only in relation to the velocity normal to the leading edge, but also to the wing section and incidence in a plane normal to the leading edge. The normal section is of about 9.25 per cent maximum thickness and of a section differing appreciably, as shown in Fig.32, from the streamwise section which is 6 per cent RAE 101; the normal plane incidence is approximately half the streamwise value. The critical Mach number at zero incidence for the normal section is estimated to be about 0.74 compared to 0.81 for the 6 per cent RAE 101 section, and the values at incidence are very much less. Conditions normal to the leading edge can therefore be expected to be supercritical at low incidence even at the lowest supersonic Mach number $M = 1.42$ where the Mach number normal to the leading edge is 0.70 approximately.

Static pressure distributions for two dimensional flow over an unswept wing are frequently presented (for example in Ref.5) in the form of the ratio p/H against x/c , H being the stagnation pressure. For a swept wing it appears appropriate to plot, for the flow in a section normal to the leading edge, p/H_n against x_n/c_n , where H_n is the stagnation pressure for

for the flow normal to the leading edge, and x_n and c_n also relate to the normal section. The results for the upper surface of the swept wing at $\alpha = 10$ degrees are presented in this way for the three supersonic speeds, in Fig.33; they were obtained by cross plotting from the isobar diagrams. The curves obtained are of similar form to those for two-dimensional flow⁵, with little change, as Mach number is varied, in the pressure at a fixed point upstream of the shock, the position of which moves back with Mach number in two fairly regular steps. The local Mach number in front of the shock in a direction normal to the leading edge (which is also approximately normal to the shock in the central region of the wing) is however rather higher than for comparable two dimensional flow conditions, being about 2.0 compared, for example, to 1.4 to 1.5 for a 10 per cent RAE 104 section at incidences of 4 and 6 degrees¹³; the local resultant Mach number in front of the shock on the swept wing for the range of main stream velocities considered varies from 2.3 to 2.7 approximately.

An assessment of conditions behind the shock and at the trailing edge can be made in the way used by Pearcey⁵ in discussing two dimensional transonic flow on aerofoils. Pearcey's work shows that the shock position and pressure recovery through the shock are very much affected by the interaction of the shock wave with the surface boundary layer. In particular, when the incidence of a thin aerofoil is increased at a fixed transonic Mach number, the terminating shock of the supersonic region on the upper surface moves rearward and increases in strength, until this is sufficient to separate the wing boundary layer; this separation reduces the pressure recovery through the shock wave. Pearcey has suggested that if the incidence is further increased until the pressure recovery is insufficient to re-establish subsonic conditions after the shock, there is a rapid expansion of the separation bubble downstream of the shock. At this stage in the flow development, the rearward movement of the shock is halted and it moves forward with further increase in incidence. Separation of the flow on the upper surface extending beyond the trailing edge results in pressure recovery to the free stream value being delayed to near the point downstream of the trailing edge where the separation bubble closes; in consequence the pressures on the upper and lower surfaces of the aerofoil equalise at the trailing edge at a value below the free stream level. Pearcey suggests therefore that when the pressure behind the shock falls below the sonic value (and rapid expansion of the bubble occurs) the trailing edge pressure diverges from the free stream value. A marked divergence of the trailing edge pressure is possible when supersonic conditions extend to the trailing edge, for the pressures on the two surfaces can then equalise with a supersonic expansion from the lower surface.

In the curves in Fig.33, the pressure has fallen below the sonic value behind the shock at all three speeds, and apparently below the sonic value at the trailing edge for $M = 1.61$ and 1.82 but less definitely so at $M = 1.42$, for which the pressure is increasing fairly rapidly towards the trailing edge; marked separation extending to the trailing edge is therefore indicated at $M = 1.61$ and 1.82 . It is questionable however whether a satisfactory assessment of trailing edge conditions can be made in terms of conditions normal to the leading edge, and consideration of conditions normal to the trailing edge may be preferable. Further analysis of the results on this basis is to be made, particularly for low incidence conditions at $M = 1.42$, where, from the pressure records (Fig.19), it appears that there is a change from attached to separated flow at the trailing edge between 2 and 4 degrees; also that the trailing edge pressure falls below the sonic value at about 4 degrees. At higher incidences there is a supersonic expansion from the lower to the upper surface to equalise the pressures at the trailing edge.

An attempt has been made to determine the local Mach number at which shock induced separation first occurs. Generally the stage at which separation first occurs does not coincide with a condition at which pressure and oil flow records were taken, but on the best evidence available from these records, it appears that the local Mach number normal to the leading edge at which separation first occurs is about 1.6 compared to 1.22 to 1.26 in two dimensional flow¹⁴. Estimates have also been made of p_2/p_1 , the pressure ratio across the shock for separation, which is essentially a measure of the shock strength; at $M = 1.61$, the values at the two outer pressure stations range from 1.15 to 1.35 before separation and from 1.6 to 2.2 after separation. These figures are consistent with the value $p_2/p_1 = 1.40$ which Pearcey quotes for separation in two dimensional flow⁵.

The few illustrative examples given here are only an indication of the order of magnitude of some of the significant parameters in the flow; a general systematic analysis would be required before definite conclusions can be drawn from the results about the relationship of the flow on swept wings to that on unswept wings. This is more difficult because of the relative complexity of the wing form, and it would be preferable, in attempting to assess the effect of sweepback, to start if possible with an experimental correlation of the characteristics of a yawed two dimensional wing with those of the same wing unyawed at lower speeds. It would also be of interest to investigate the characteristics of an untapered swept wing of relatively large aspect ratio to isolate end effects to some extent from the central part of the wing.

9.3 Interpretation of oil flow patterns

Confidence in the interpretation of oil flow pictures is strengthened by the correlation found between inferences made from certain features of the oil patterns, and flow characteristics determined from pressure records. The main points for which this has been possible are summarised below.

In the oil pictures for $M = 0.81$, for example $\alpha = 8$ degrees in Fig.5, a region of unmoved oil near the leading edge indicates a leading edge separation bubble, and this is confirmed by the presence of flattened regions in the pressure distributions in Fig.4⁴. Behind the unmoved oil region, lines in a spiral form with a heavily scoured central or axial region are interpreted as a part-span vortex running diagonally across the wing behind the separation bubble, and this is also shown by the presence of secondary suction peaks in the pressure distribution. A notable feature of a number of the subsonic oil pictures (including Fig.5) is an array of minor vortex type patterns at the leading edge, but the pressure stations are too widely spaced for correlation with these patterns.

The first oil pictures obtained at supersonic speed are difficult to interpret because of distortion which occurred during the tunnel shutdown stage. At 4 degrees at $M = 1.61$, for example, (Fig.11), there is a rough oil line, in a position not closely related to any special feature of the flow, which cannot be reliably interpreted; the position of the line should in accordance with the evidence at other incidences, approximate to that of the wing shock, and the discrepancy in this case might be due to some difference in the test conditions, or possibly to distortion during shutdown of the tunnel. Other pictures, such as $\alpha = 10$ degrees at $M = 1.61$ in Fig.15, show a cleared line; this is a line along which oil was observed to collect when the wing was at the test incidence, and from which it cleared only when the incidence was reduced to zero. The line therefore appears to mark the definite forward boundary

of a separation region at which some of the oil comes to rest, and correlation with the pressure records shows the line to be of similar shape to, and to lie just behind the wing shock. In later tests when the incidence was not reduced to zero for shutdown, the forward boundary of this shock induced separation region is shown on the flow picture as a well defined oil line, as for example at $\alpha = 10$ degrees at $M = 1.82$ in Fig.27; this line gives a close indication to the shock position determined from pressure measurements. This is the type of oil pattern that should normally be achieved and if time had permitted, the tests at $M = 1.61$ would have been repeated without reduction of incidence at the shutdown stage.

The separation region, of which the oil line is the forward boundary, may be of widely variant extent. It can vary from a small closed bubble, possibly for example just aft of the oblique leg of the shock to a separation extending back over the trailing edge over the outer part of the wing. An extensive region of flow separation behind the shock is shown by less marked development of the oil than in front of it, with oil lines running in an approximately spanwise direction and in some cases turning forward towards the shock; confirmation of separation extending to the trailing edge from oil indications of this kind has been obtained in the pressure records from deviation of the trailing edge pressure from the free stream value.

The correspondence obtained between the oil patterns and pressure records in the subsonic and later supersonic tests, shows that assessment of the main characteristics of the flow from oil pictures can be reasonably straightforward when marked distortion during the shutdown stage is avoided. It is generally helpful in interpreting an oil pattern to know the way in which it developed, but observation of the development clearly becomes desirable when there is a possibility of significant distortion. The achievement of definitely shaped oil patterns with a minimum of distortion depends on a number of practical points of technique, and these are to be discussed in a later note dealing generally with the oil method of flow visualisation.

10 Conclusions

The pressure measurements and oil flow observations at $M = 0.81$ show typical subsonic flow characteristics for a swept wing, with a leading edge separation towards the tip and a part-span vortex, growing in extent as incidence is increased from about 6 degrees upwards. On the basis of these results, a physical picture (more complete than seems previously to have been given) is suggested of the flow with a part span vortex. The oil pictures show in some cases an array of minor vortex patterns at the leading edge, which appear to be an underlayer effect.

The results at $M = 1.61$ show a compression shock extending inwards over the wing as incidence is increased; a notable feature of the shock development is the appearance at 8 degrees and more strongly at 10 degrees of an oblique leg on the shock, inclined forward towards the leading edge, and adjoining the outer approximately spanwise shock line near mid-span. Shock induced separation is shown spreading from the tip inwards as incidence is increased, and the outer part of the shock also curves forward towards the leading edge in the tip region, because of the forward movement associated with separation. There are indications behind the oblique leg of the shock at higher incidences of a vortex flow, analogous in some ways to the part span vortex of subsonic flow.

The results at $M = 1.42$ and 1.82 show similar characteristics to those at $M = 1.61$, but the outer portion of the shock on the wing is further forward at the lower speed and further aft at the higher speed than at $M = 1.61$.

The presence of a main wing shock is an essentially transonic characteristic, and the flow depends apparently on a subsonic component of the mainstream velocity. An approximate assessment of the flow conditions in terms of the velocity component normal to the leading edge shows that the flow conditions are supercritical above zero incidence at the lowest supersonic speed tested, as observed experimentally. The position of the outer shock is determined by the requirement for pressure recovery by the trailing edge, while the oblique leg effects re-alignment of the flow relative to the wall.

From a limited analysis of the results, the velocity distribution over an approximately mid span section normal to the leading edge is similar in form to that for two dimensional transonic flow. The local Mach number normal to the leading edge for separation is higher than found in two dimensional tests, but the pressure ratio across the shock for separation appears to be consistent with the two dimensional value.

Correlation with the pressure records has shown that satisfactory assessment of flow characteristics can be made from surface oil patterns; when the oil pattern cannot be recorded while the tunnel is running, however, observation of the development of the pattern is desirable for reliable interpretation, if marked distortion is possible at the shutdown stage.

List of Symbols

c	wing section chord parallel to plane of symmetry
\bar{c}	mean aerodynamic chord
C_p	$\frac{p - p_o}{q}$
H	stagnation pressure
H_n	pressure for stagnation in a direction normal to the wing leading edge
M	Mach number
p	static pressure
p_o	free stream static pressure
p_1	shock upstream pressure
p_2	shock downstream pressure
q	free stream dynamic pressure, $\frac{1}{2}\rho V^2$
R	Reynold's number, $\rho \bar{V}c/\mu$
s	wing half span
V	free stream velocity
x	distance from leading edge along chord parallel to plane of symmetry
x_n	distance from leading edge along chord normal to leading edge

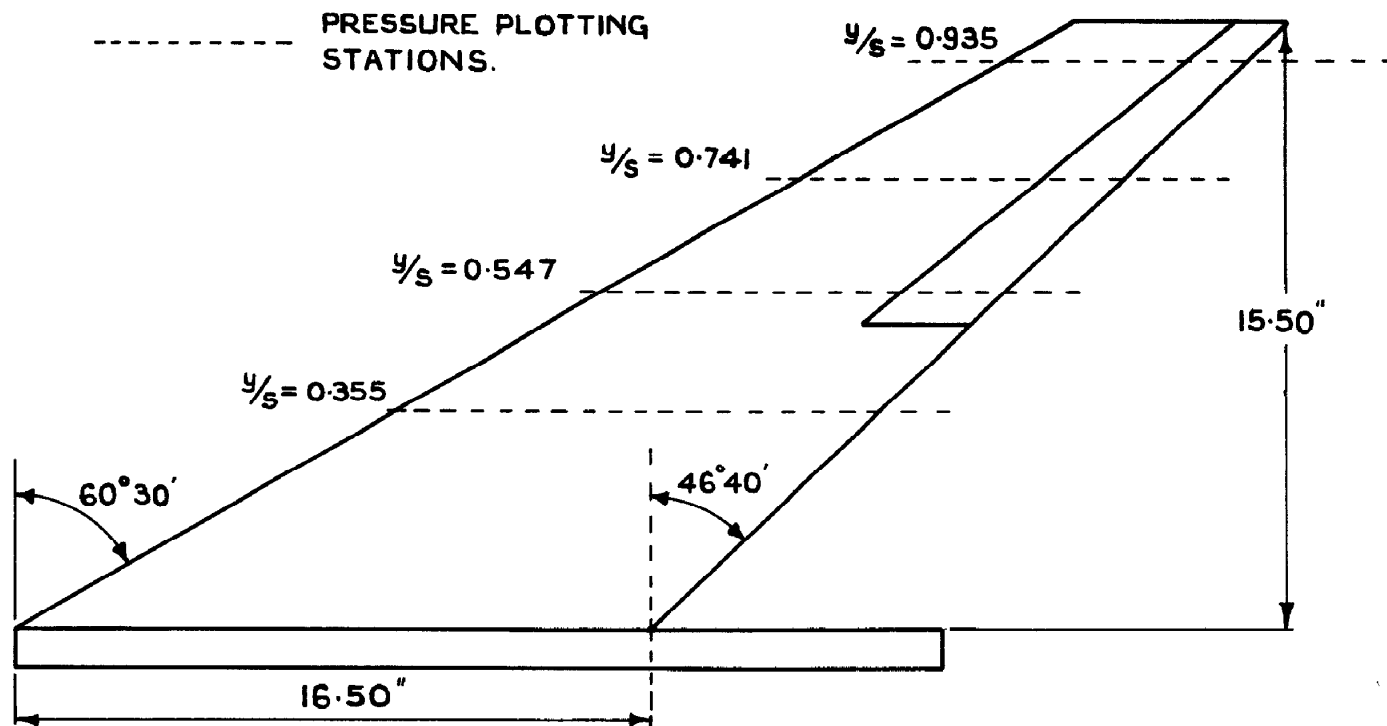
y distance from plane of symmetry
 α wing incidence
 μ viscosity coefficient of air in free stream
 ρ density of air in free stream

REFERENCES

<u>No.</u>	<u>Author</u>	<u>Title, etc.</u>
1	Morris, D.E.	Calibration of the flow in the working section of the 3 ft x 3 ft tunnel, National Aeronautical Establishment C.P. No.261. Sept. 1954
2	Winter, K.G. Scott-Wilson, J.B. and Davies, F.V.	Methods of determination and of fixing boundary layer transition on wind tunnel models at supersonic speeds O.P. No.212. Sept. 1954
3	Herriot, J.G.	Blockage corrections for three dimensional flow in closed throat wind tunnels, with consideration of the effect of compressibility NACA Report No.995 1950
4	Küchemann, D.	Types of flow on swept wings with special reference to free boundaries and vortex sheets Journal Royal Aeronautical Society 1953, Vol.57, No.683
5	Pearcey, H.H.	Some effects of shock induced separation of turbulent boundary layers in transonic flow past aerofoils Proc. of Symposium on boundary layer effects in aerodynamics, Paper 9, N.P.L., March, 1955 R & M.3108.
6	Bickley, W.G.	Critical conditions for compressible flow R & M.2330. May, 1946
7	Küchemann, D.	The effects of viscosity on the types of flow on swept wings Proc. of Symposium on boundary layer effects in aerodynamics, Paper 6, N.P.L. March, 1955 (to be published by H.M.S.O.)
8	Norbury, T.F. and Crabtree, L.F.	A simplified model of the incompressible flow past two dimensional aerofoils with a long bubble type of flow separation ARC 17945. June, 1955
9	Neumark, S.	Critical Mach numbers for thin untapered swept wings at zero incidence R & M.2821. Nov. 1949
10	Küchemann, D.	A simple method of calculating the span and chordwise loading on straight and swept wings of any given aspect ratio at subsonic speeds R & M.2935. August, 1952

REFERENCES (Contd)

<u>No.</u>	<u>Author</u>	<u>Title, etc.</u>
11	Whitcomb, R.T. and Kelly, T.C.	A study of the flow over a 45° sweptback wing fuselage combination at transonic Mach numbers NACA RM L52D01 NACA/TIB/3215 1952
12	Solomon, W. and Schmeer, J.W.	Effect of longitudinal wing position on the pressure characteristics at transonic speeds of a 45° swept- back wing fuselage model NACA RM L52K05a NACA/TIB/3654 March, 1953
13	Rogers, E.W.E. Berry, C.J. and Cash, R.F.	Tests at high subsonic speeds on a 10 per cent thick pressure plotting aerofoil of RAE 104 section. Part II Pressure distributions and flow photographs R & M.2863. Feb. 1951
14	Holden, D.W. Pearcey, H.H. and Gadd, G.E. Seddon, J.	The interaction between shock waves and boundary layers With a note on: The effects of the interaction on the performance of supersonic intakes C.P. No.180. 1954



PERCENTAGE CHORDWISE POSITION OF PRESSURE HOLES.			
$y/s = 0.355$	$y/s = 0.547$	$y/s = 0.741$	$y/s = 0.935$
10	4	4	4
20	8	8	8
30	12	12	12
40	16	16	16
50	20	20	28
60	28	28	36
68	36	36	44
76	44	44	52
84	52	52	59
92	56	59	66
	60	66	73
	64	73	77
	68	77	83
	72	83	89
	77	89	
	80	95	
	84		
	88		
	92		
	96		

WING TAPER RATIO 0.333
 ASPECT RATIO 2.828
 AERODYNAMIC MEAN CHORD 12.25 INS.
 CONTROL 0.5 SEMISPAN, 25% CHORD.

AEROFOIL SECTION : 6% R.A.E. 101. STREAMWISE
 MAX. THICKNESS POINT. 31% CHORD
 TRAILING EDGE ANGLE 6.13°
 LEADING EDGE RADIUS 0.002749 C

FIG. I. DETAILS OF MODEL

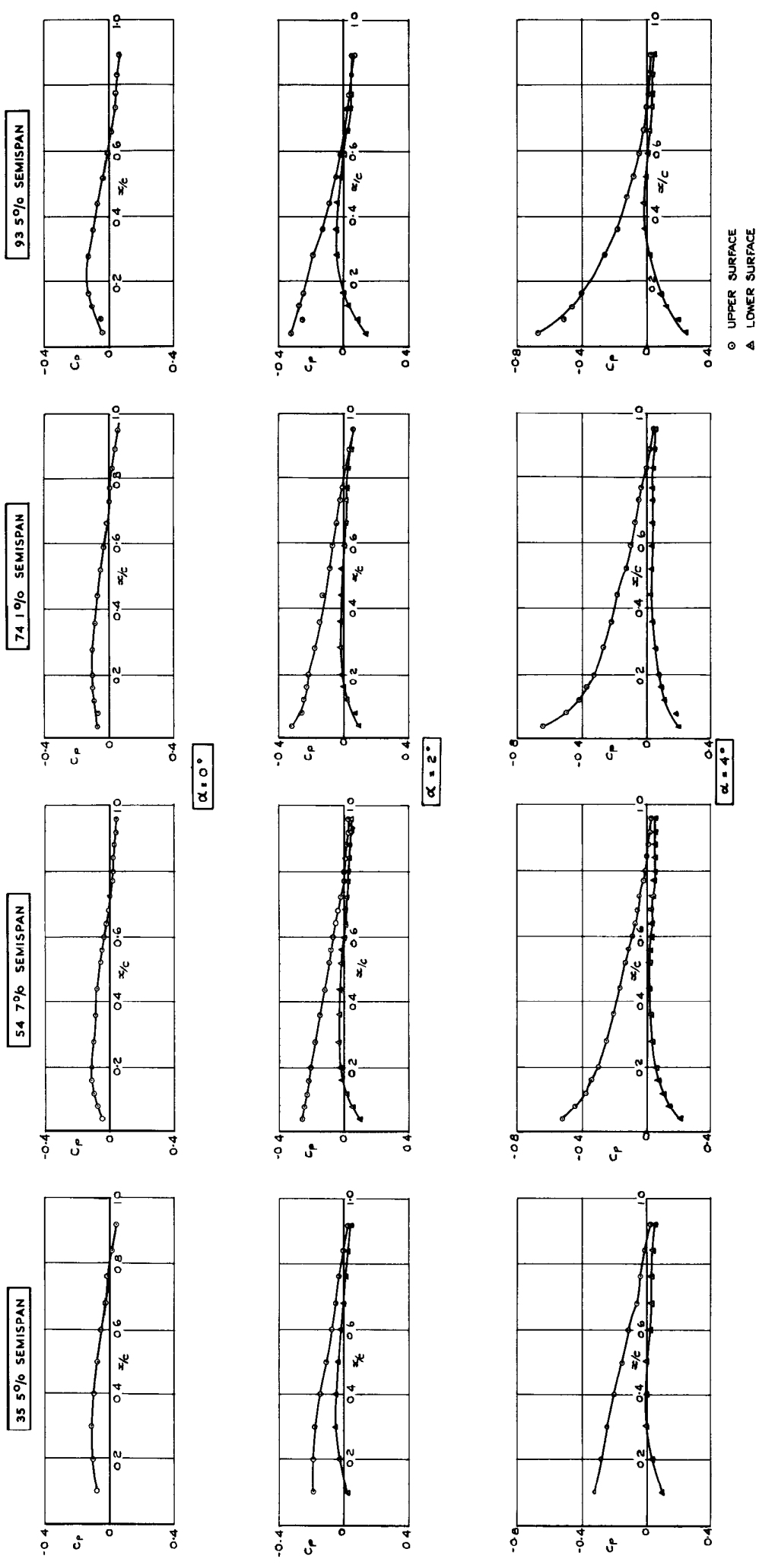


FIG. 2. CHORDWISE PRESSURE DISTRIBUTIONS FOR WING INCIDENCES $\alpha = 0, 2$ AND 4 DEGREES AT $M = 0.81$: $RE. No. = 4.43 \times 10^6$

THE ARROWS INDICATE THE SPANWISE POSITIONS OF THE PRESSURE STATIONS

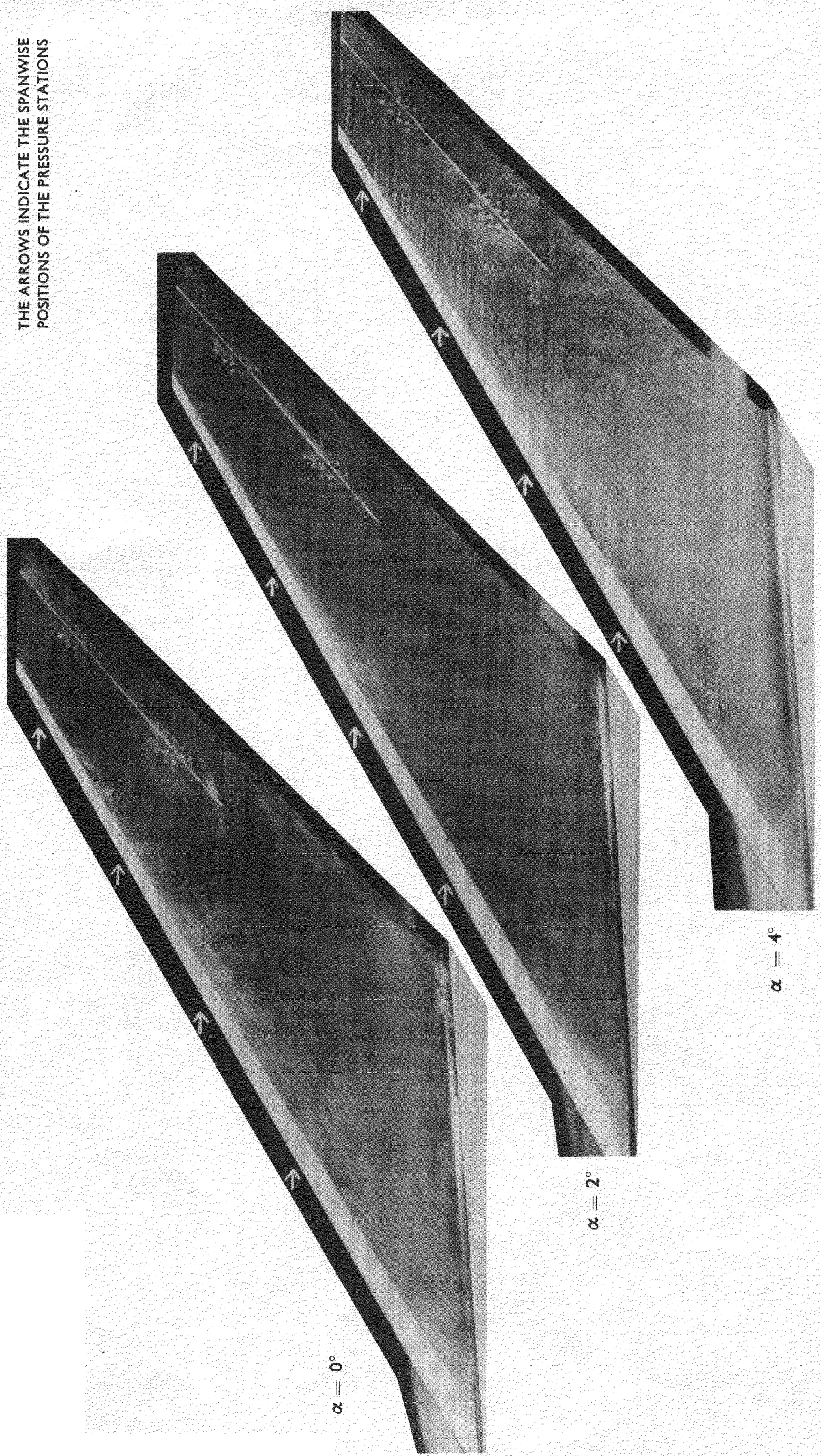


FIG.3. OIL FLOW OBSERVATIONS ON UPPER SURFACE FOR WING INCIDENCES
 $\alpha = 0,2,4^\circ$ AT $M = 0.81$; $Re No. = 4.43 \times 10^6$

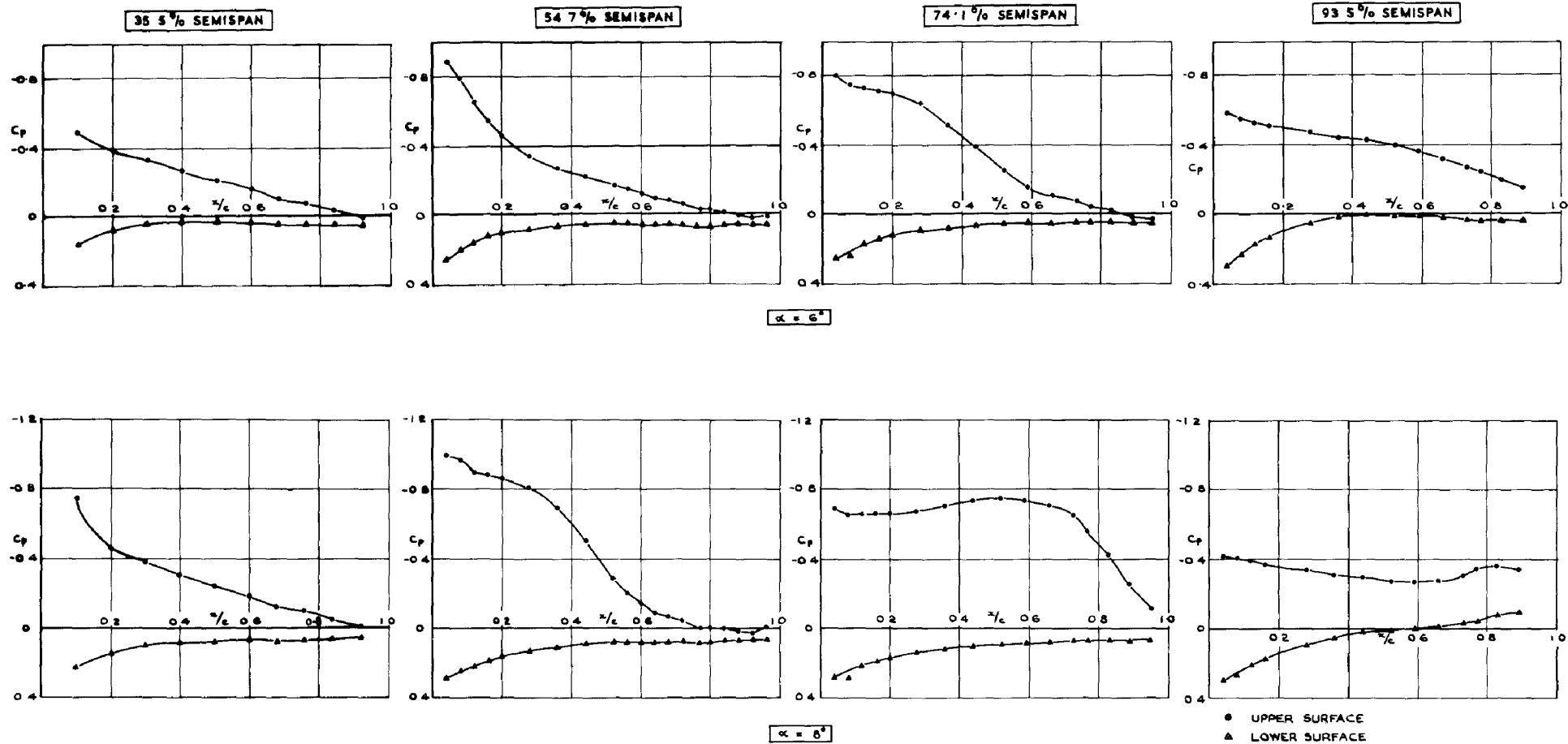
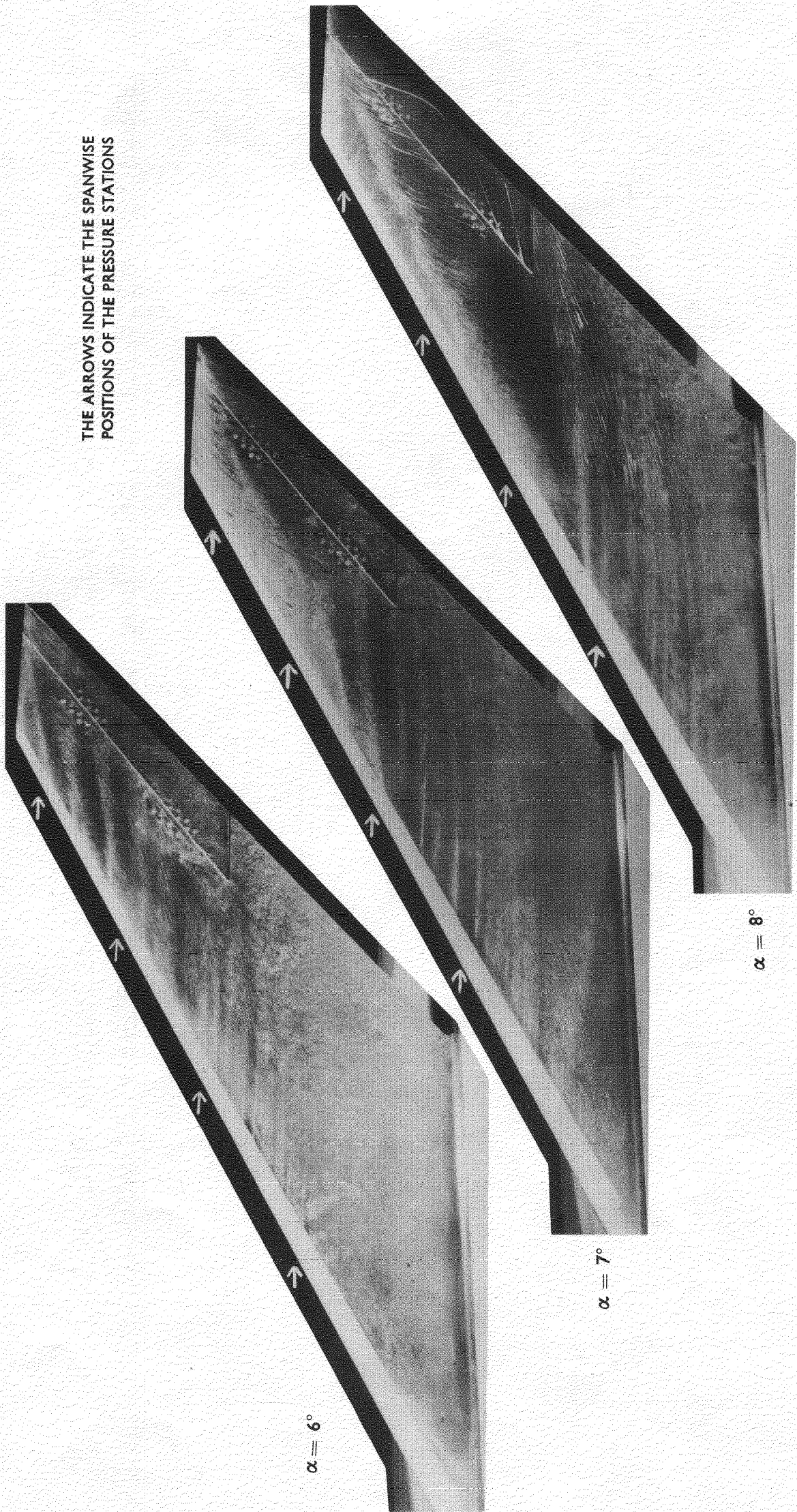
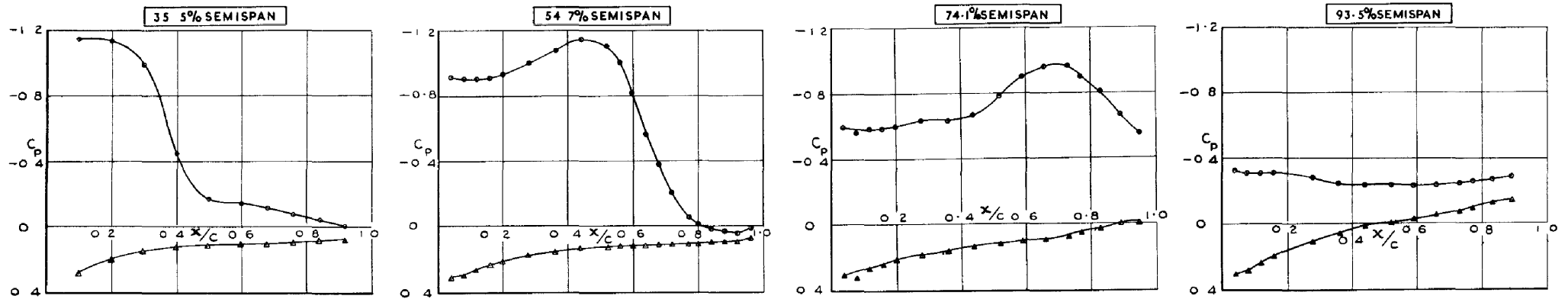


FIG. 4. CHORDWISE PRESSURE DISTRIBUTIONS FOR WING INCIDENCES $\alpha = 6.8$ DEGREES AT $M = 0.81$; $Re. No. = 4.43 \times 10^6$

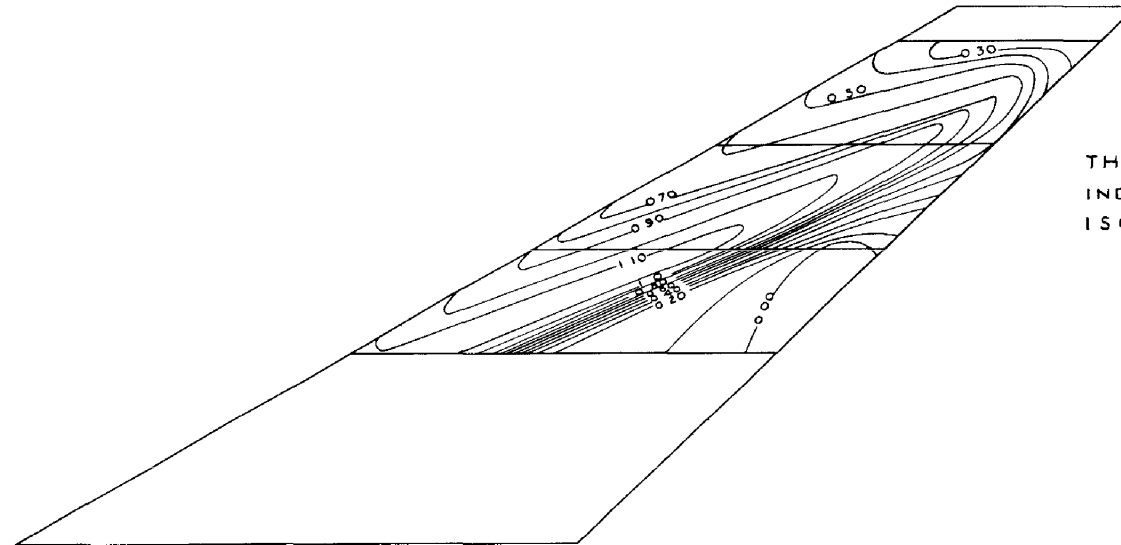


THE ARROWS INDICATE THE SPANWISE POSITIONS OF THE PRESSURE STATIONS

FIG.5. OIL FLOW OBSERVATIONS ON UPPER SURFACE FOR WING INCIDENCES
 $\alpha = 6,7,8^\circ$ AT $M = 0.81$; Re.No. = 4.43×10^6

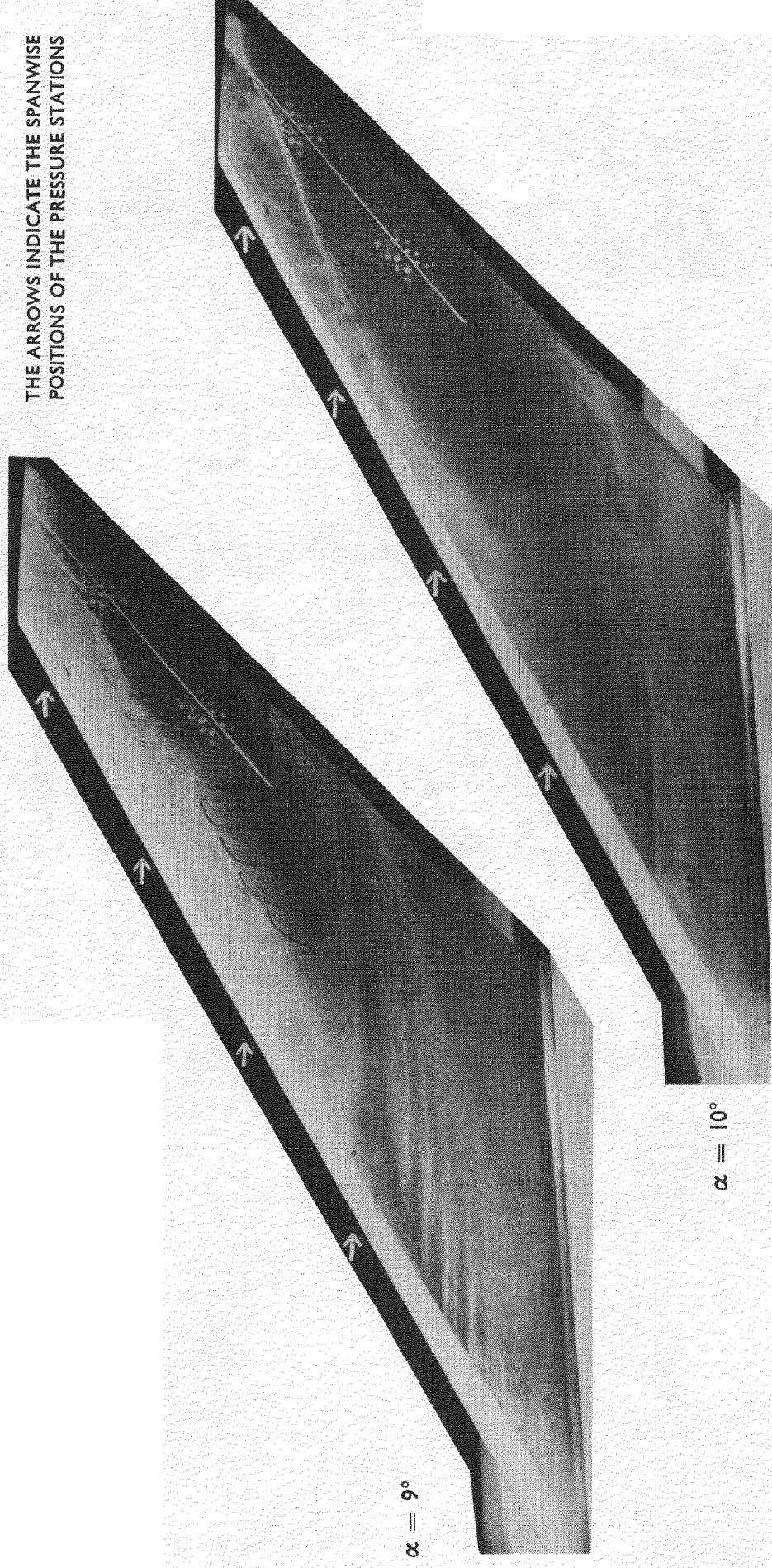


○ UPPER SURFACE
 ▲ LOWER SURFACE



THE PARAMETER
 INDICATED ON THE
 ISOBARS IS $-C_p$

FIG.6. CHORDWISE PRESSURE DISTRIBUTIONS FOR WING INCIDENCE $\alpha = 10$ DEGREES
 AT $M = 0.81$ & CORRESPONDING ISOBAR DIAGRAM FOR UPPER SURFACE;
 $Re. No. 4.43 \times 10^6$



THE ARROWS INDICATE THE SPANWISE POSITIONS OF THE PRESSURE STATIONS

$\alpha = 9^\circ$

$\alpha = 10^\circ$

FIG.7. OIL FLOW OBSERVATIONS ON UPPER SURFACE FOR WING INCIDENCES $\alpha = 9, 10^\circ$ AT $M = 0.81$; $Re No. = 4.43 \times 10^6$

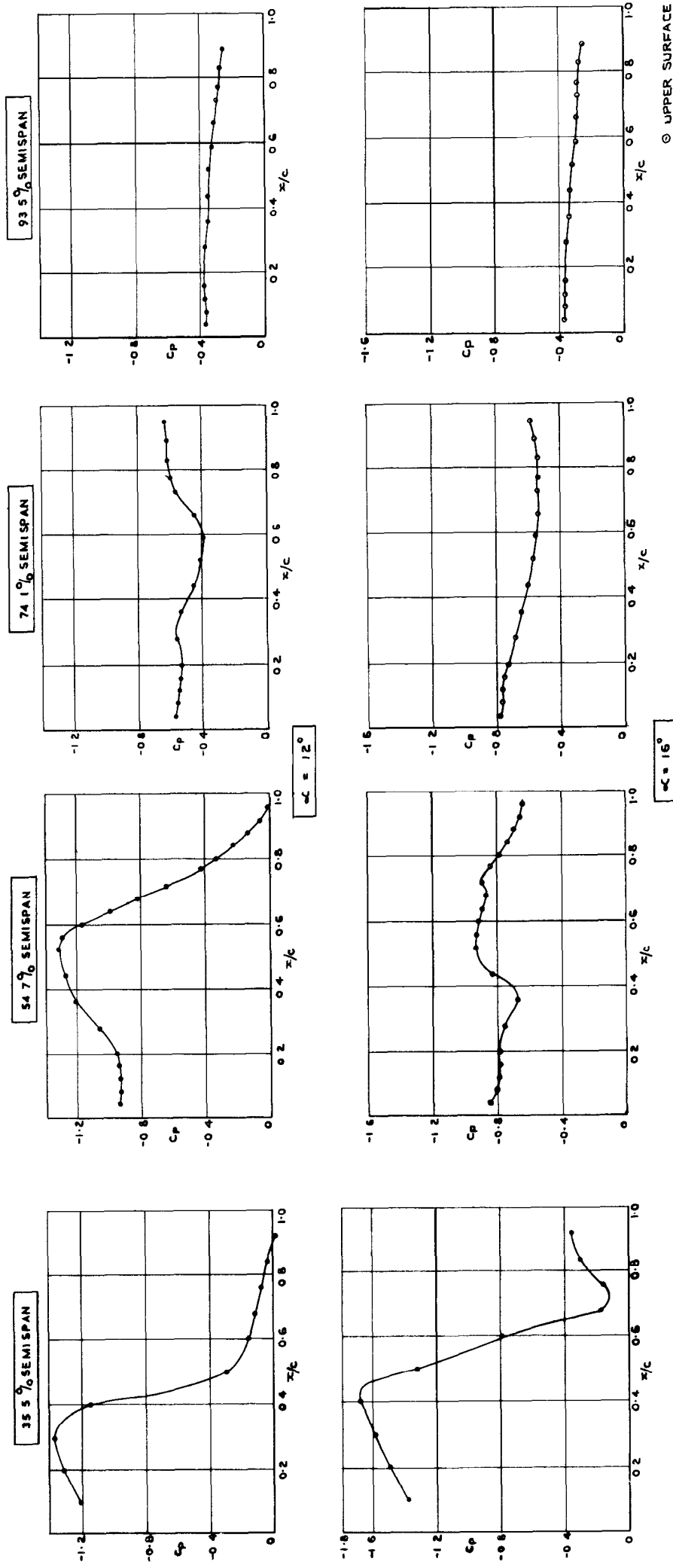
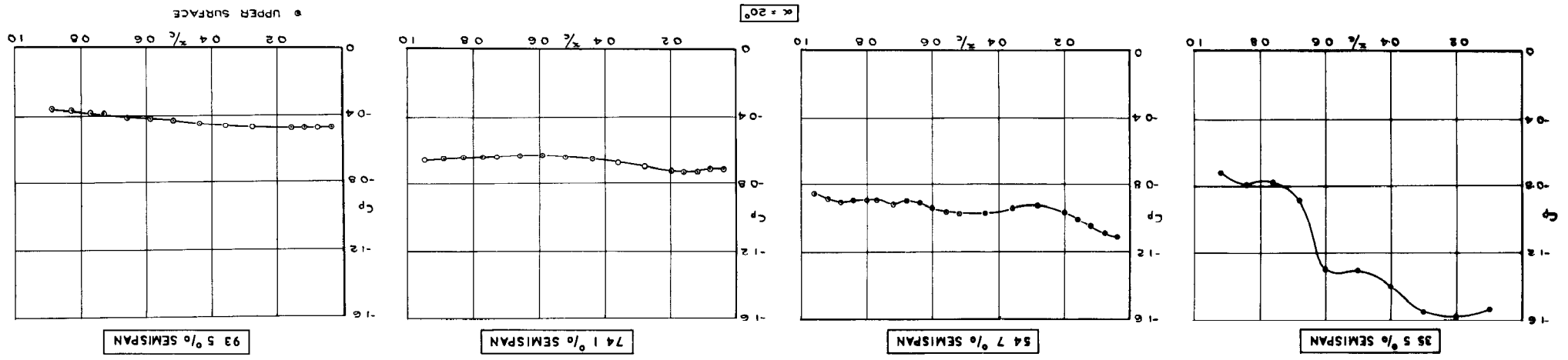
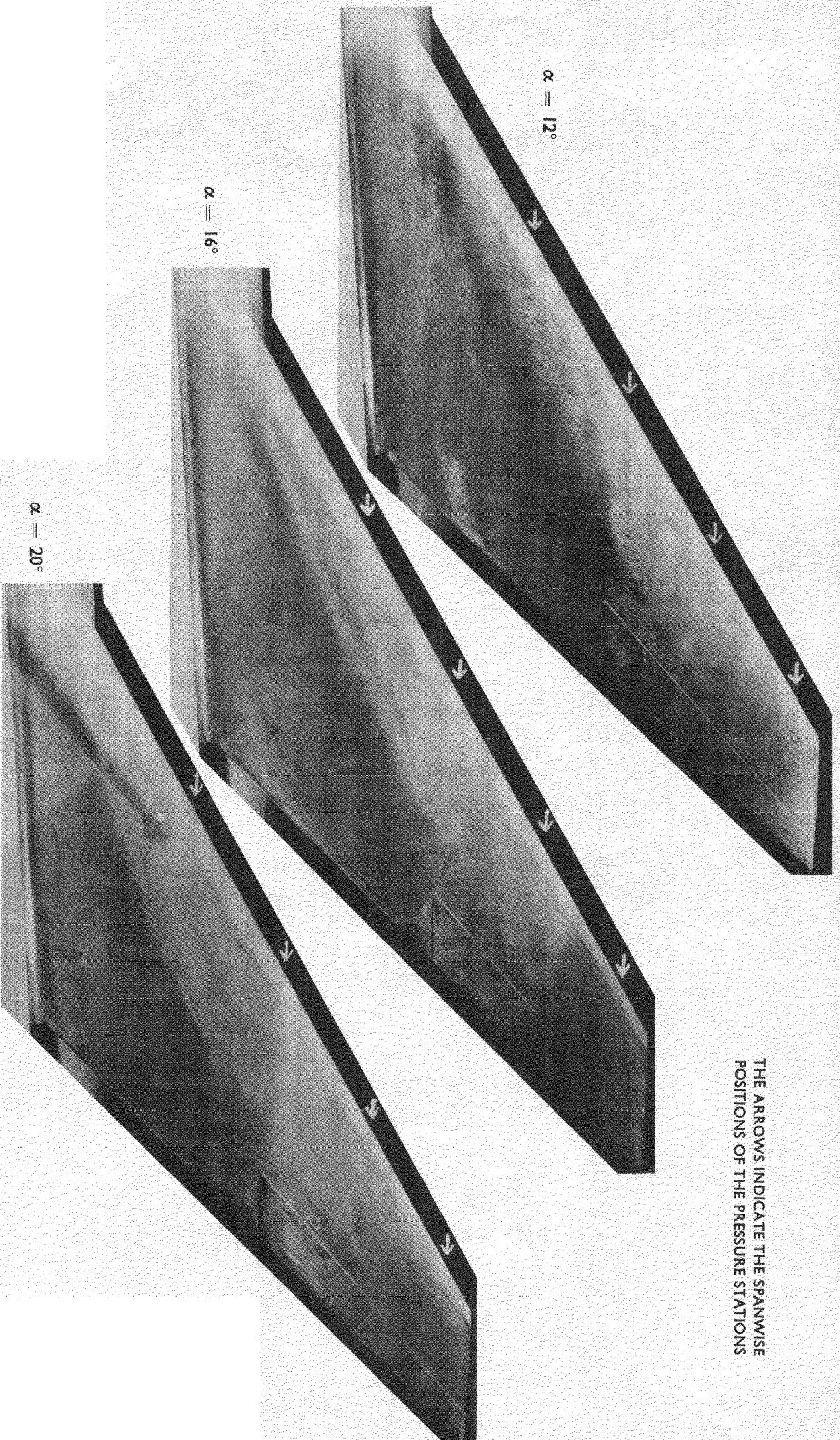


FIG. 8(a). CHORDWISE PRESSURE DISTRIBUTIONS FOR WING INCIDENCES $\alpha = 12, 16$ DEGREES AT $M = 0.81$; $RE. No. = 2.21 \times 10^6$

FIG. 8 (b). CHORDWISE PRESSURE DISTRIBUTION FOR WING INCIDENCE
 $\alpha = 20$ DEGREES AT $M = 0.81$; $Re. No. = 2.21 \times 10^6$





THE ARROWS INDICATE THE SPANWISE POSITIONS OF THE PRESSURE STATIONS

FIG.9. OIL FLOW OBSERVATIONS ON UPPER SURFACE FOR WING INCIDENCES
 $\alpha = 12, 16, 20^\circ$ AT $M = 0.81$; $Re_{No.} = 2.21 \times 10^6$

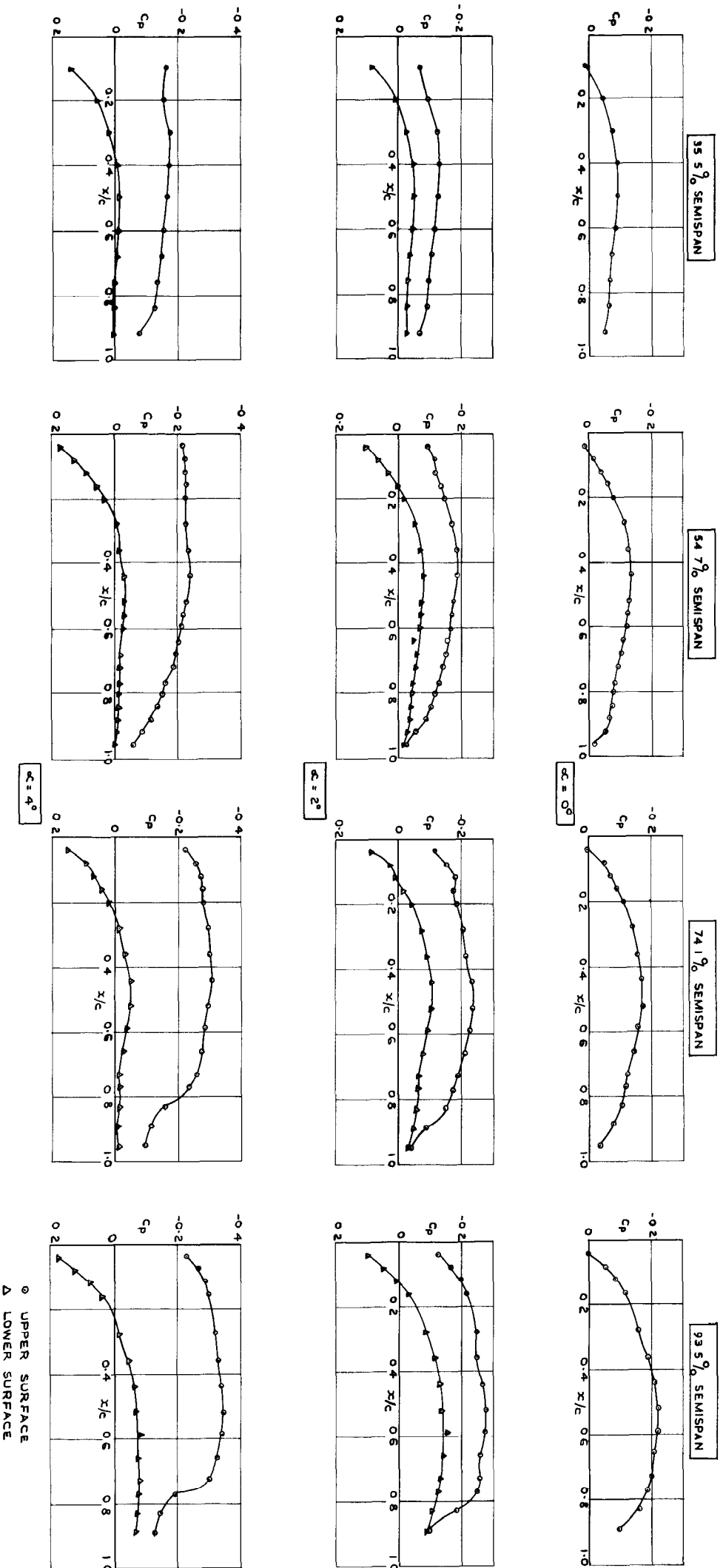


FIG. 10. CHORDWISE PRESSURE DISTRIBUTIONS FOR WING INCIDENCES $\alpha = 0, 2$ AND 4 DEGREES AT $M = 1.61$; $RE. NO. = 4.15 \times 10^6$

THE ARROWS INDICATE THE SPANWISE POSITIONS OF THE PRESSURE STATIC

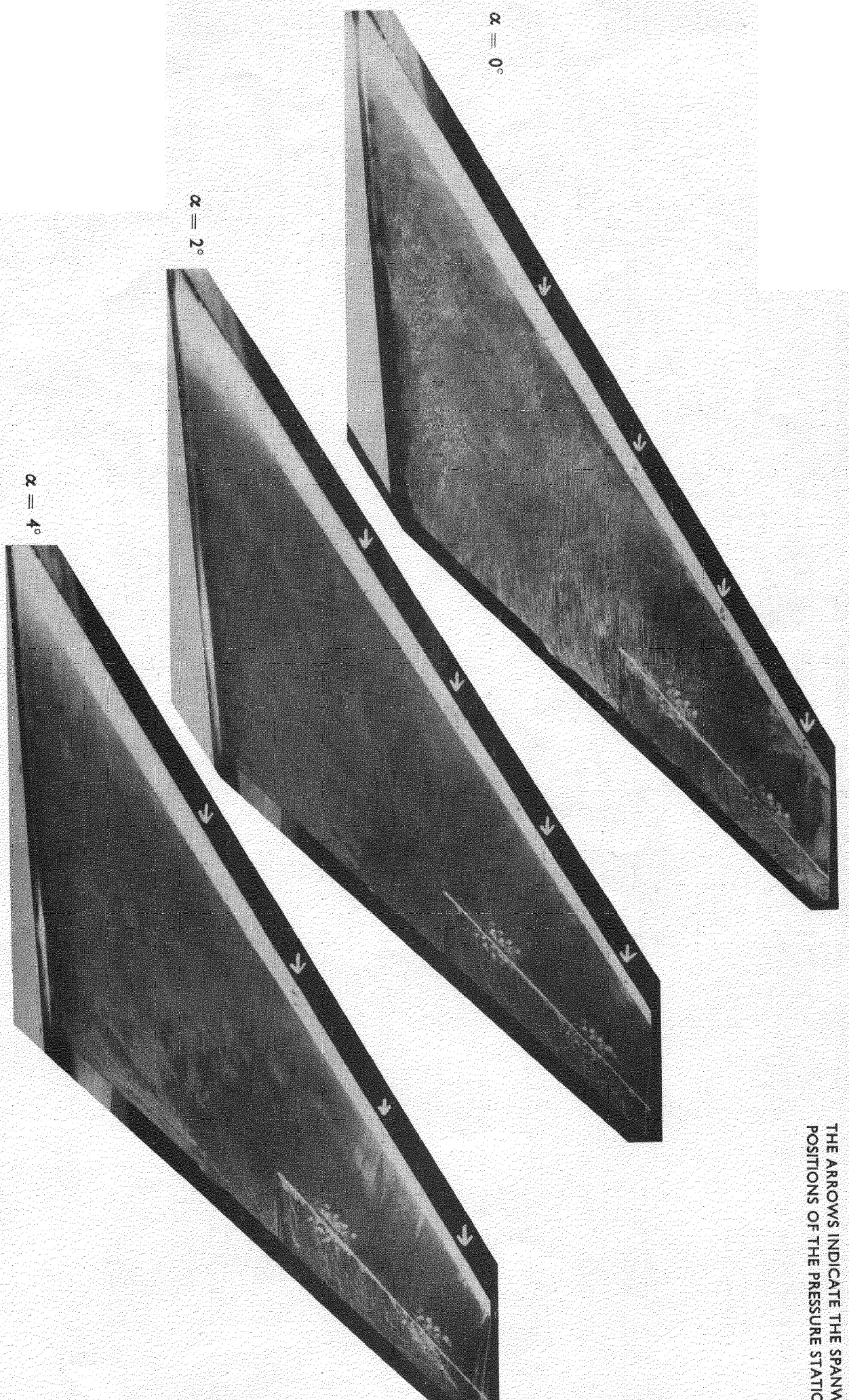
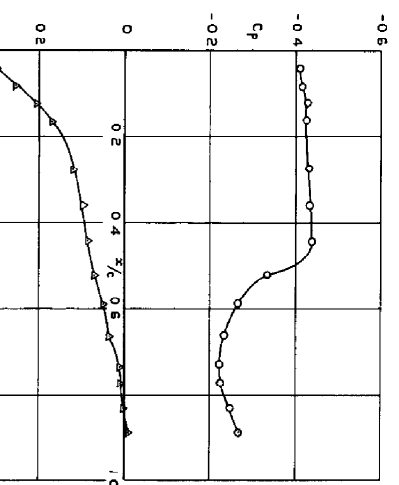
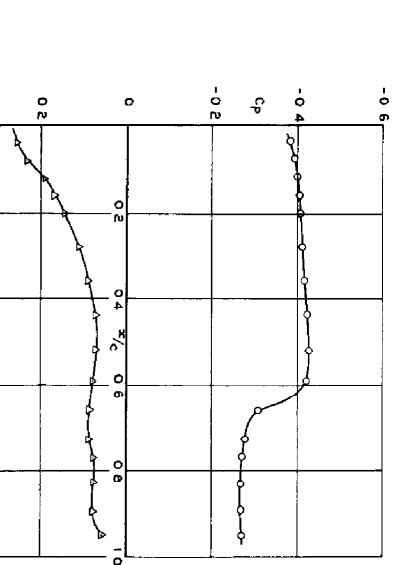
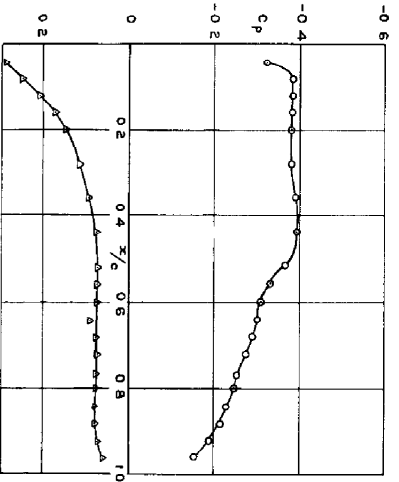
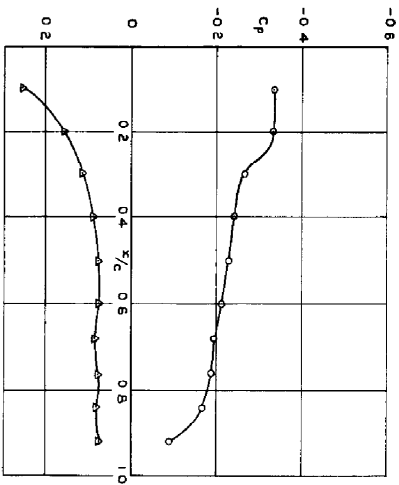
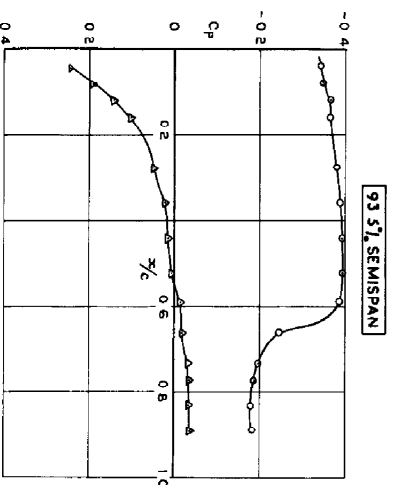
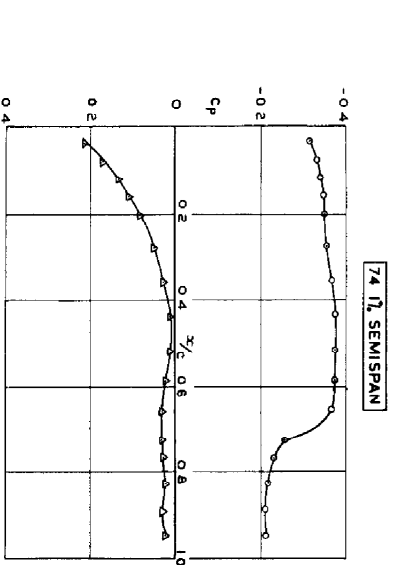
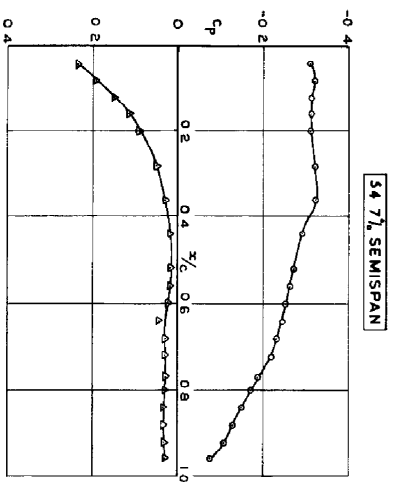
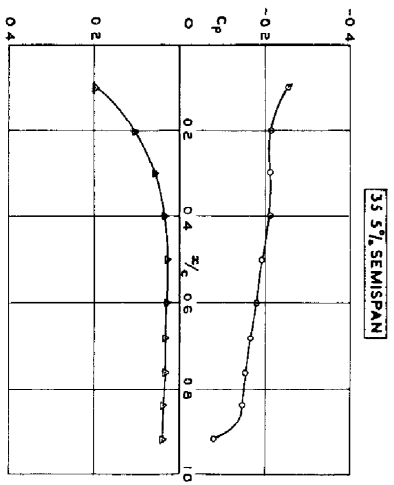
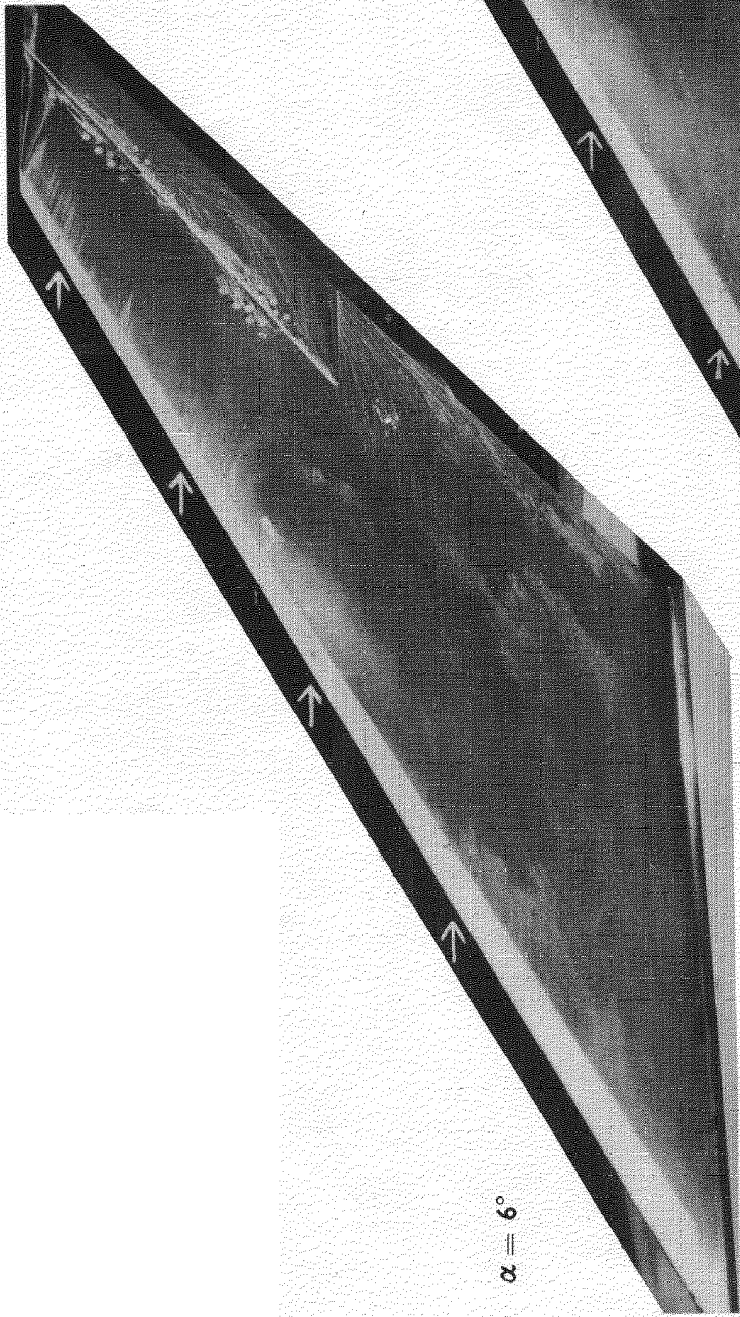


FIG.11. OIL FLOW OBSERVATIONS ON UPPER SURFACE FOR WING INCIDENCES
 $\alpha = 0, 2, 4^\circ$ AT $M = 1.61$; $Re.No. = 4.15 \times 10^6$



O UPPER SURFACE
 Δ LOWER SURFACE

FIG. 12. CHORDWISE PRESSURE DISTRIBUTIONS FOR WING INCIDENCES $\alpha = 6$,
 8 DEGREES AT $M = 1.61$; $Re. No. = 4.15 \times 10^6$



THE ARROWS INDICATE THE SPANWISE POSITIONS OF THE PRESSURE STATIONS

FIG.13. OIL FLOW OBSERVATIONS ON UPPER SURFACE FOR WING INCIDENCES
 $\alpha = 6,8^\circ$ AT $M = 1.61$; $Re No. = 4.15 \times 10^6$

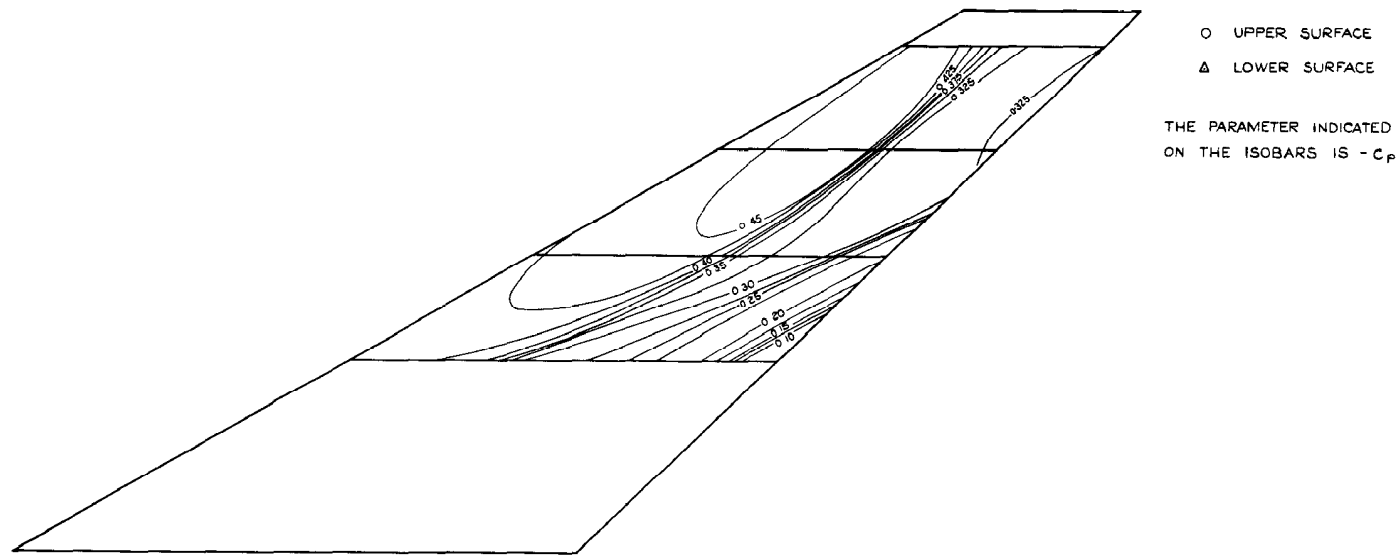
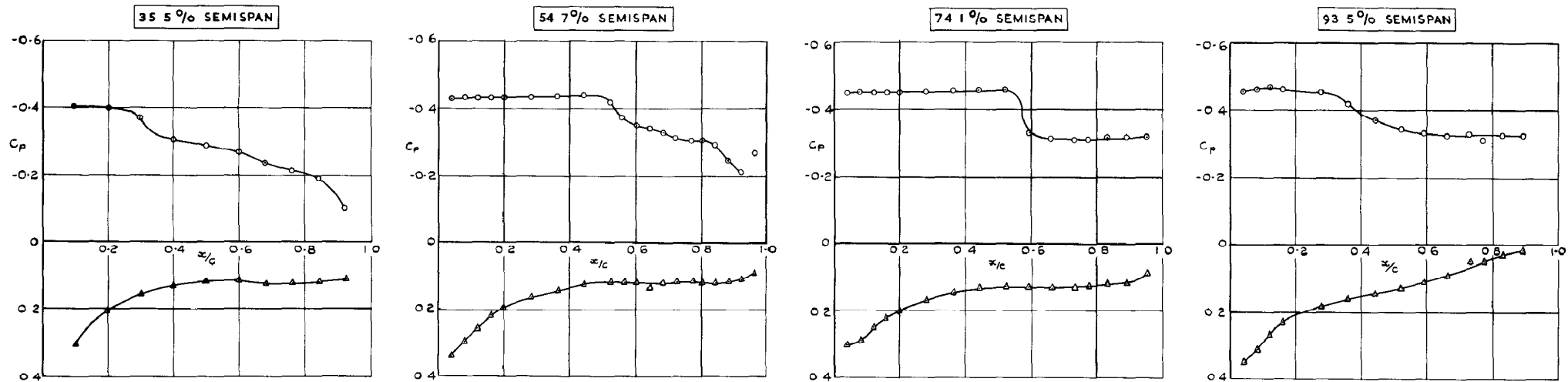


FIG. 14. CHORDWISE PRESSURE DISTRIBUTION FOR WING INCIDENCE $\alpha = 10$ DEGREES AT $M = 1.61$, AND CORRESPONDING ISOBAR DIAGRAM FOR UPPER SURFACE: $Re. No. = 4.15 \times 10^6$

THE ARROWS INDICATE THE SPANWISE
POSITIONS OF THE PRESSURE STATIONS

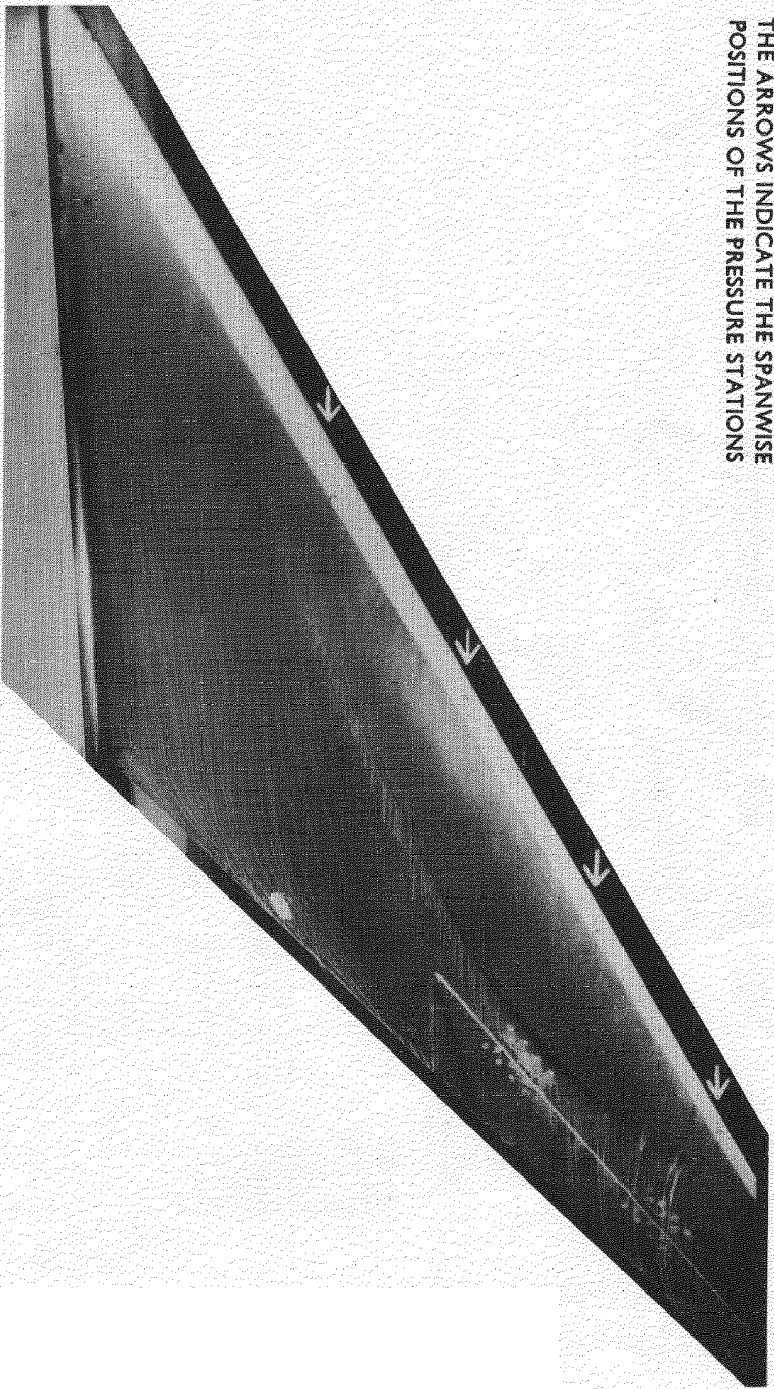


FIG.15. OIL FLOW OBSERVATION ON UPPER SURFACE FOR WING INCIDENCE
 $\alpha = 10^\circ$ AT $M = 1.61$; $Re_{No.} = 4.15 \times 10^6$

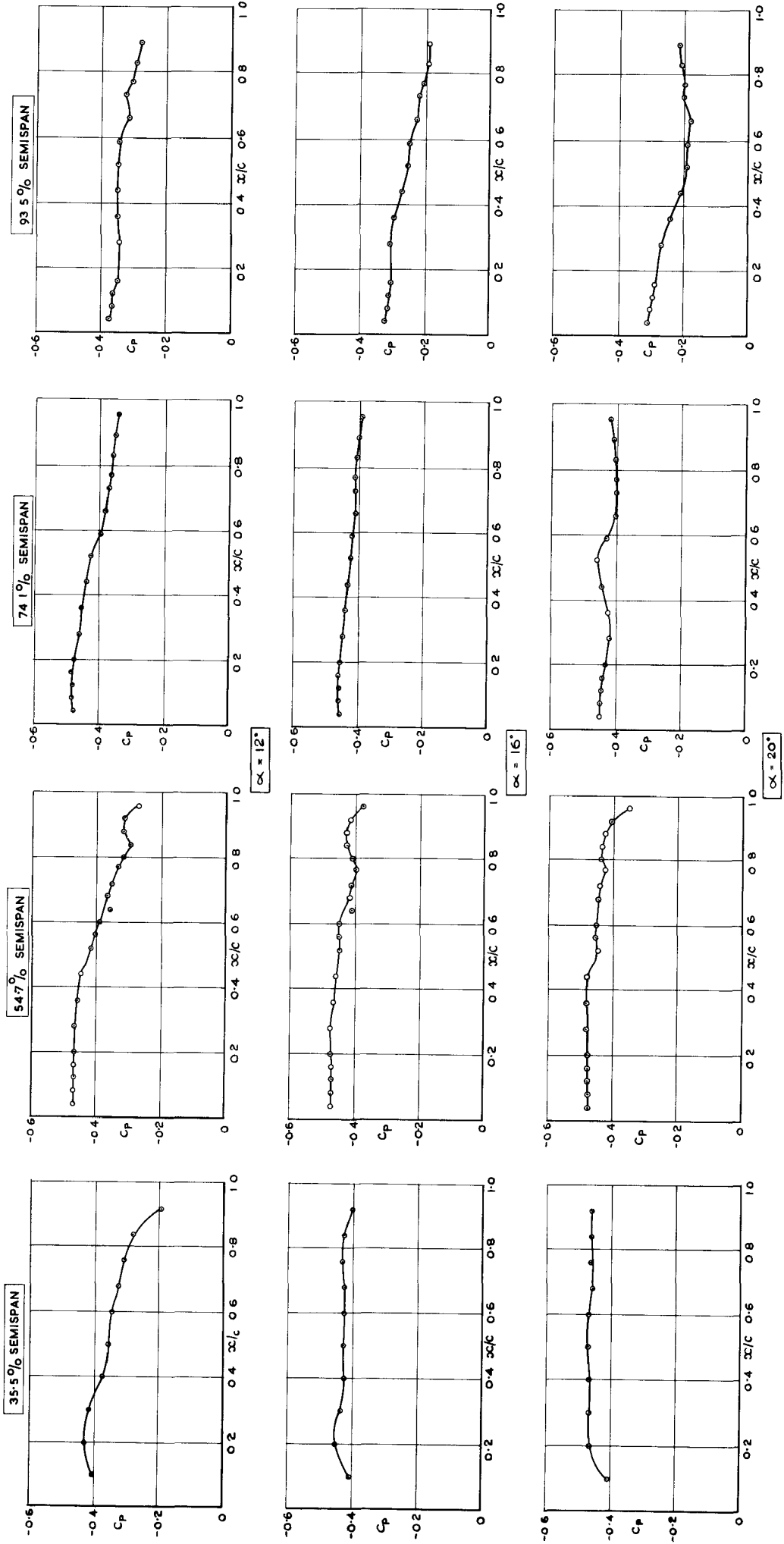


FIG. 16. CHORDWISE PRESSURE DISTRIBUTIONS FOR WING INCIDENCES $\alpha = 12, 16$ AND 20 DEGREES AT $M = 1.61$, $Re. No. = 2.07 \times 10^6$

THE ARROWS INDICATE THE SPANWISE POSITIONS OF THE PRESSURE STATIONS

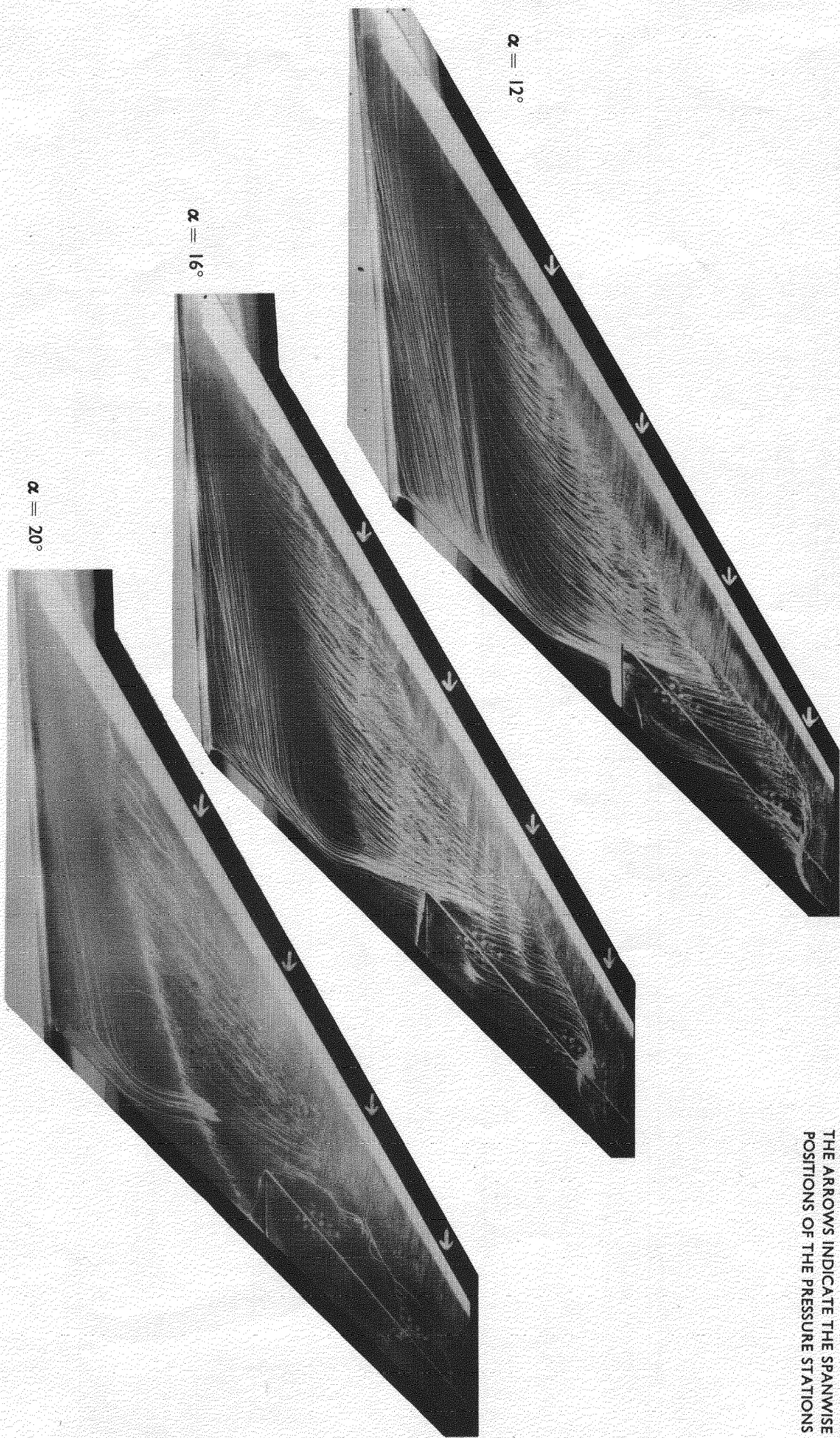
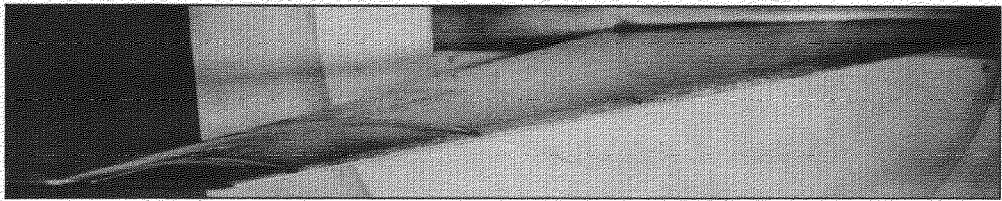
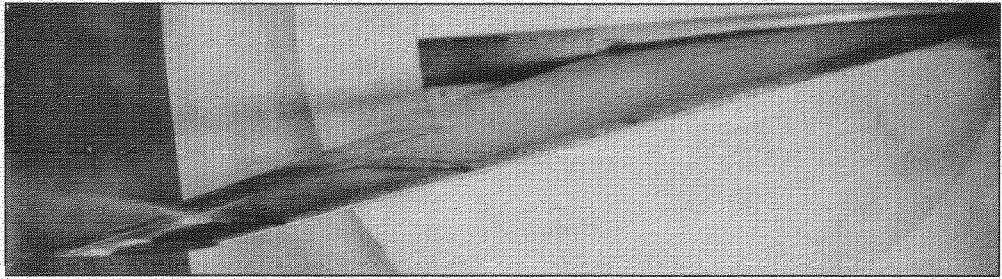


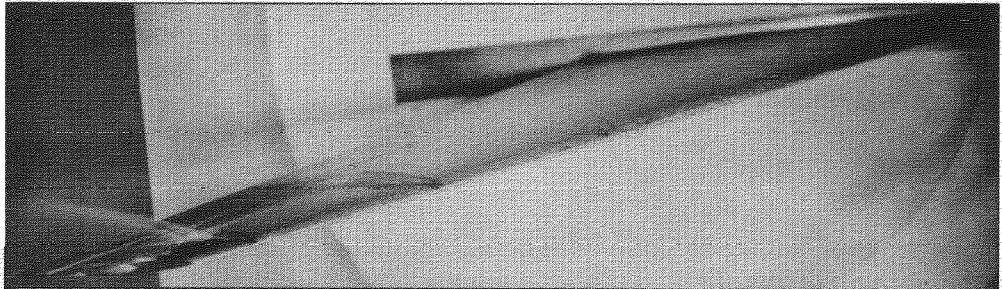
FIG.17. OIL FLOW OBSERVATIONS ON UPPER SURFACE FOR WING INCIDENCES
 $\alpha = 12, 16, 20^\circ$ AT $M = 1.61$; $Re No. = 2.07 \times 10^6$



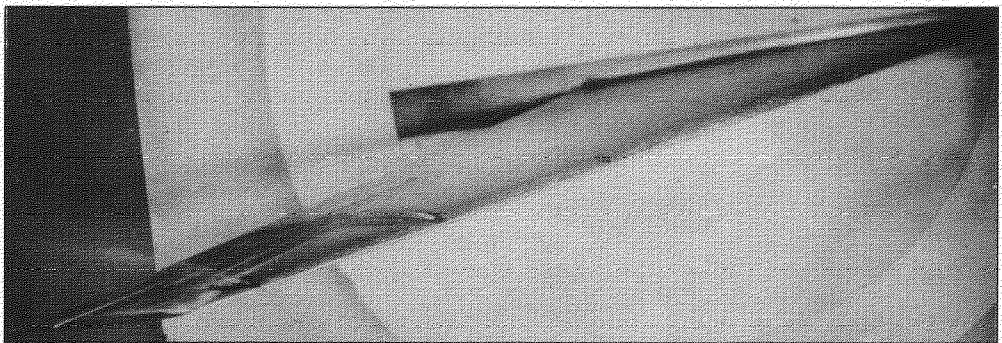
$\alpha = 2^\circ$



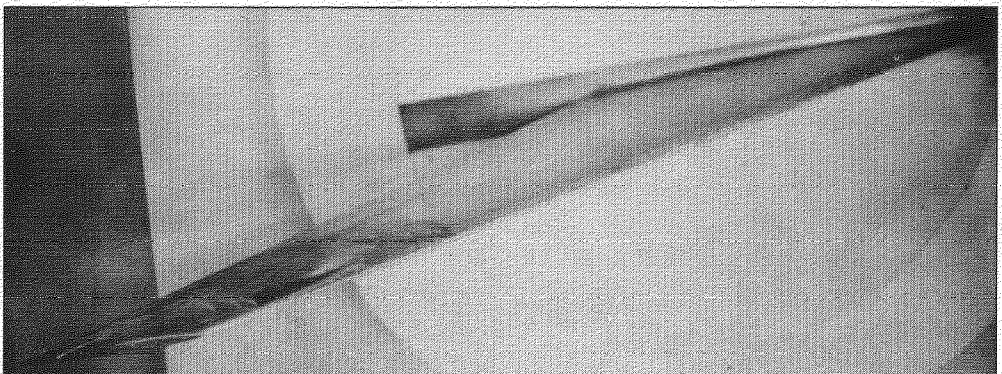
$\alpha = 6^\circ$



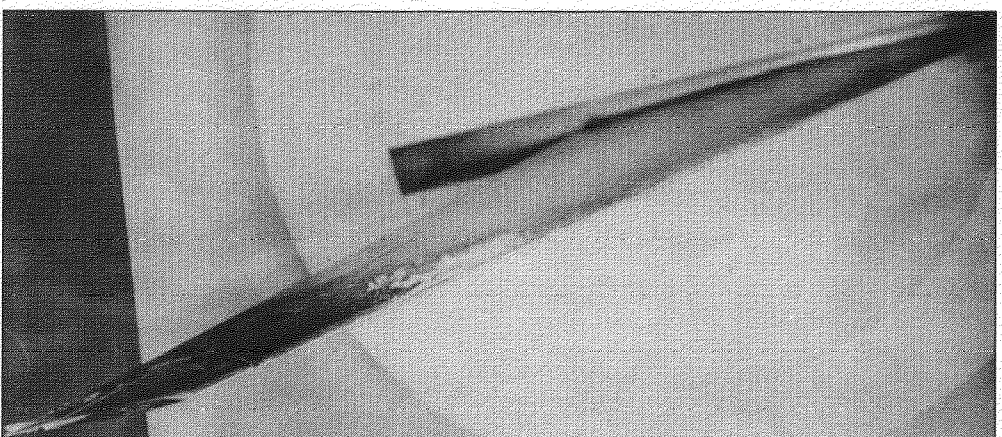
$\alpha = 8^\circ$



$\alpha = 10^\circ$



$\alpha = 12^\circ$



$\alpha = 16^\circ$

FIG.18. FLOW OBSERVATIONS RELEASING SOAP SOLUTION FROM PRESSURE HOLES ON UPPER SURFACE FOR WING INCIDENCES
 $\alpha = 2,6,8,10,12,16^\circ$ AT $M = 1.61$; Re No. = 4.15×10^6 for $\alpha \leq 10^\circ$
= 2.07×10^6 for $\alpha > 10^\circ$

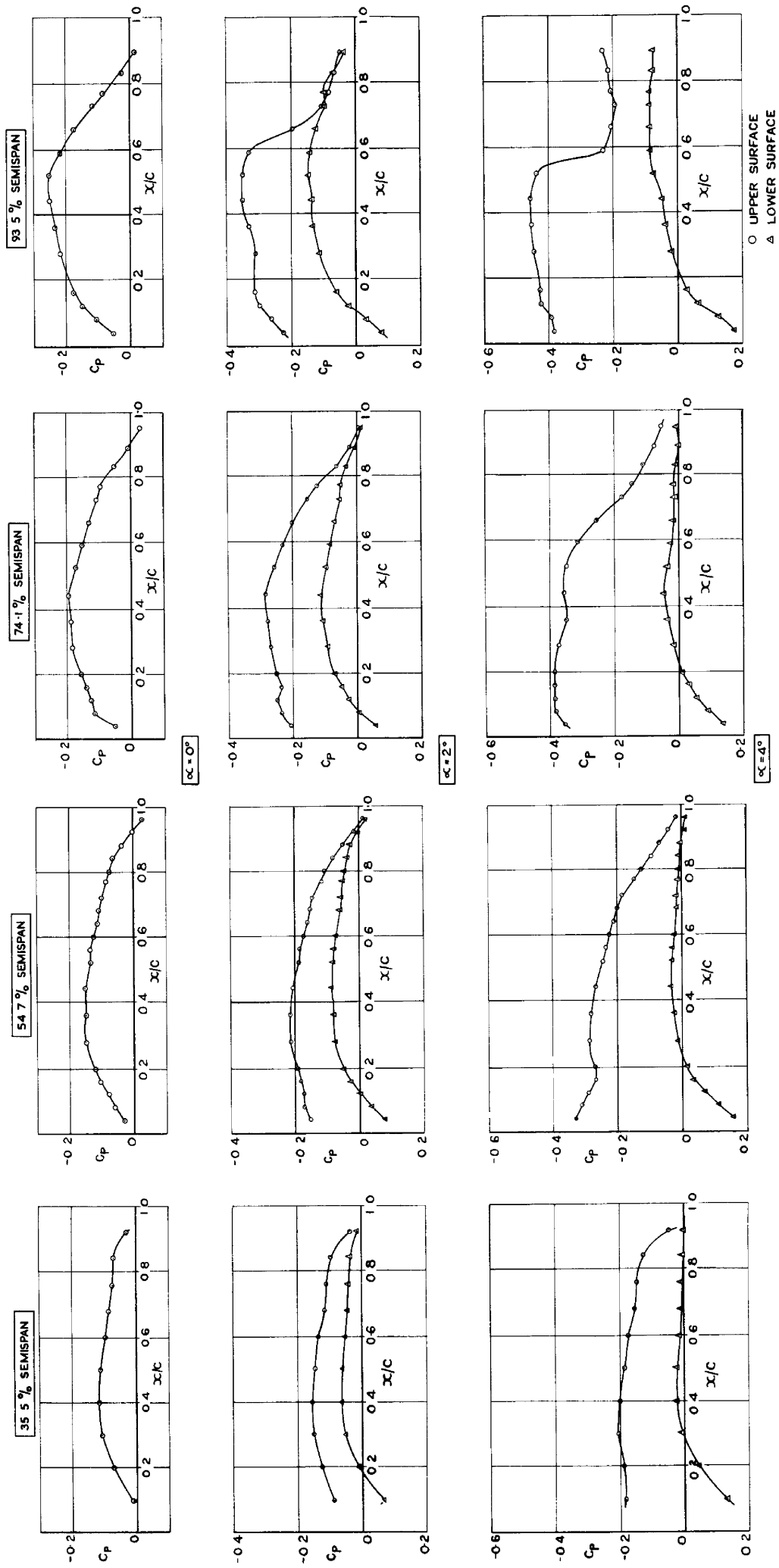


FIG. 19. CHORDWISE PRESSURE DISTRIBUTIONS FOR WING INCIDENCES

$\alpha = 0, 2$ AND 4 DEGREES AT $M = 1.42$; $Re. No. = 4.15 \times 10^6$

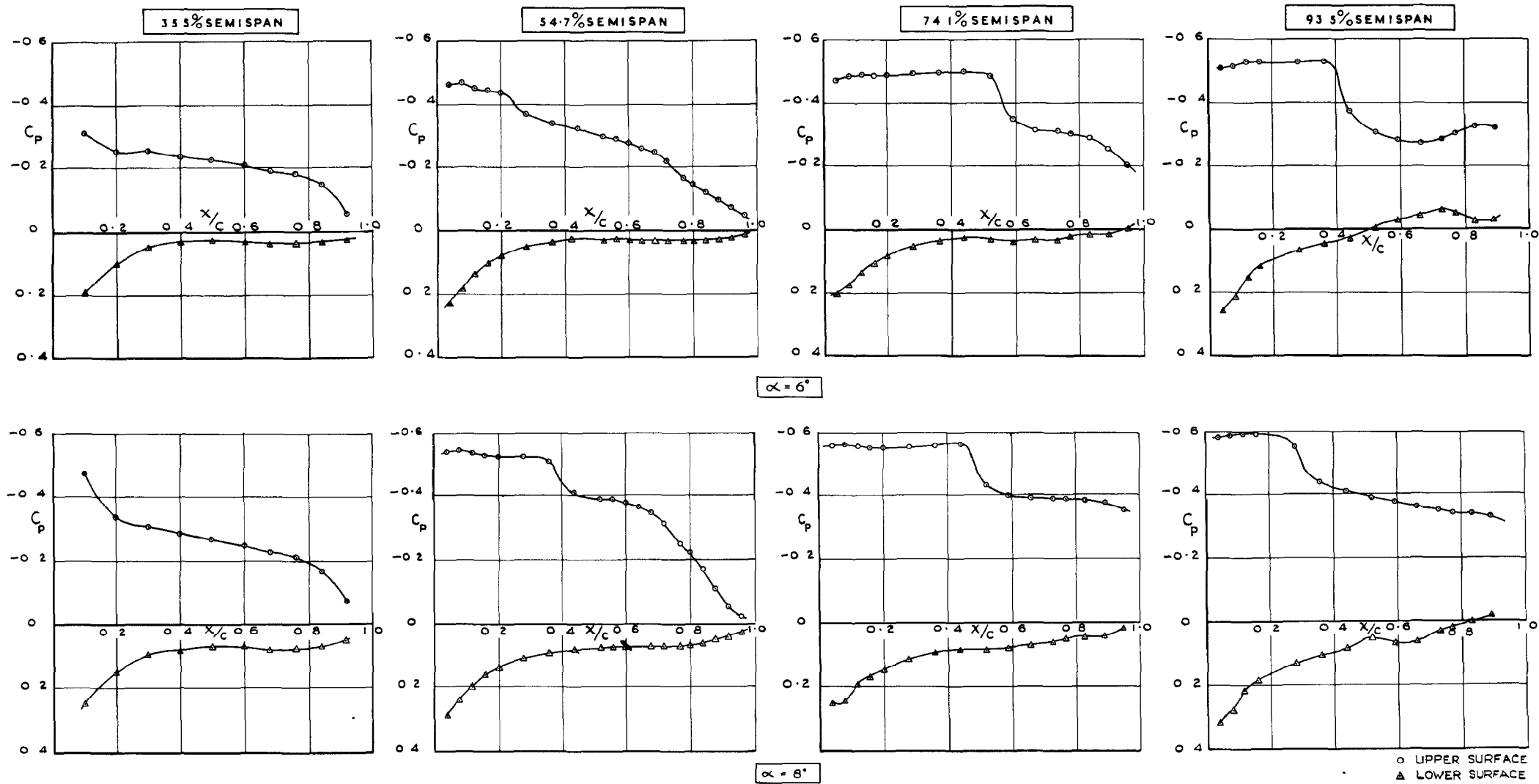


FIG. 20. CHORDWISE PRESSURE DISTRIBUTIONS FOR WING INCIDENCES $\alpha = 6, 8$ DEGREES AT $M = 1.42$; $RE. No. 4.15 \times 10^6$

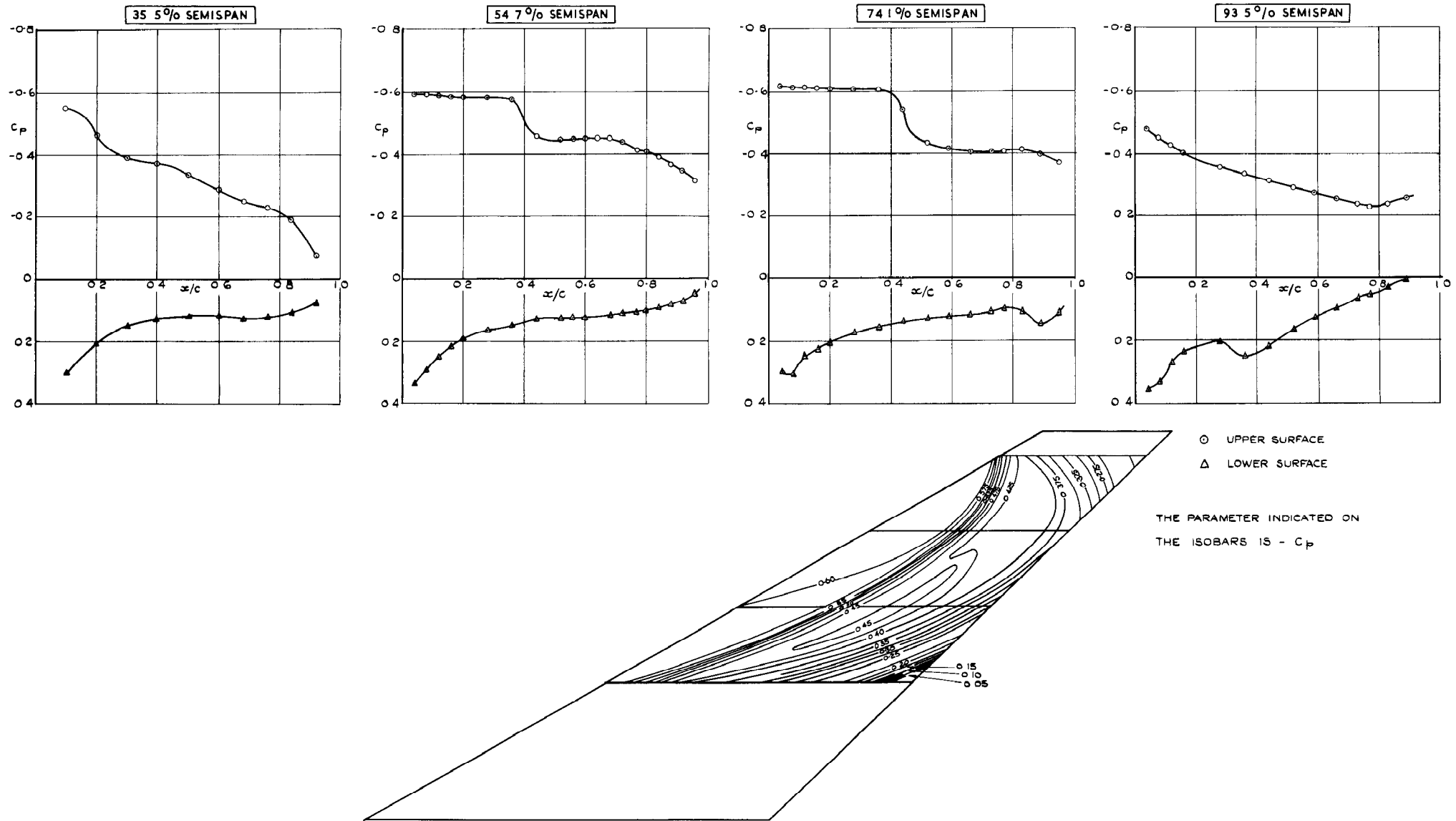
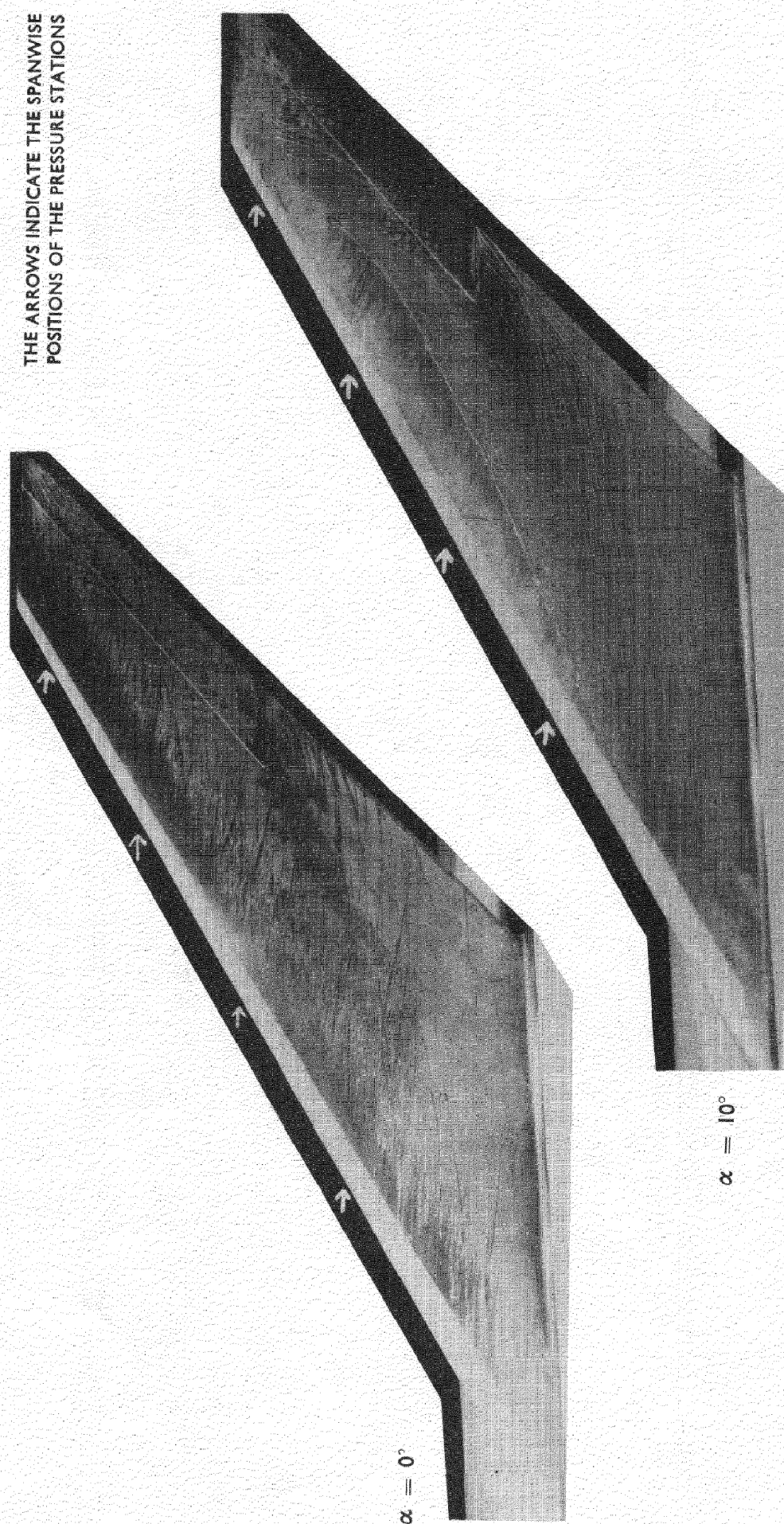


FIG. 21. CHORDWISE PRESSURE DISTRIBUTIONS FOR WING INCIDENCE $\alpha = 10$ DEGREES AT $M = 1.42$ AND CORRESPONDING ISOBAR DIAGRAM FOR UPPER SURFACE: $Re.No. = 4.15 \times 10^6$



THE ARROWS INDICATE THE SPANWISE POSITIONS OF THE PRESSURE STATIONS

FIG.22. OIL FLOW OBSERVATIONS ON UPPER SURFACE FOR WING INCIDENCES
 $\alpha = 0, 10^\circ$ AT $M = 1.42$; $Re No. = 4.15 \times 10^6$

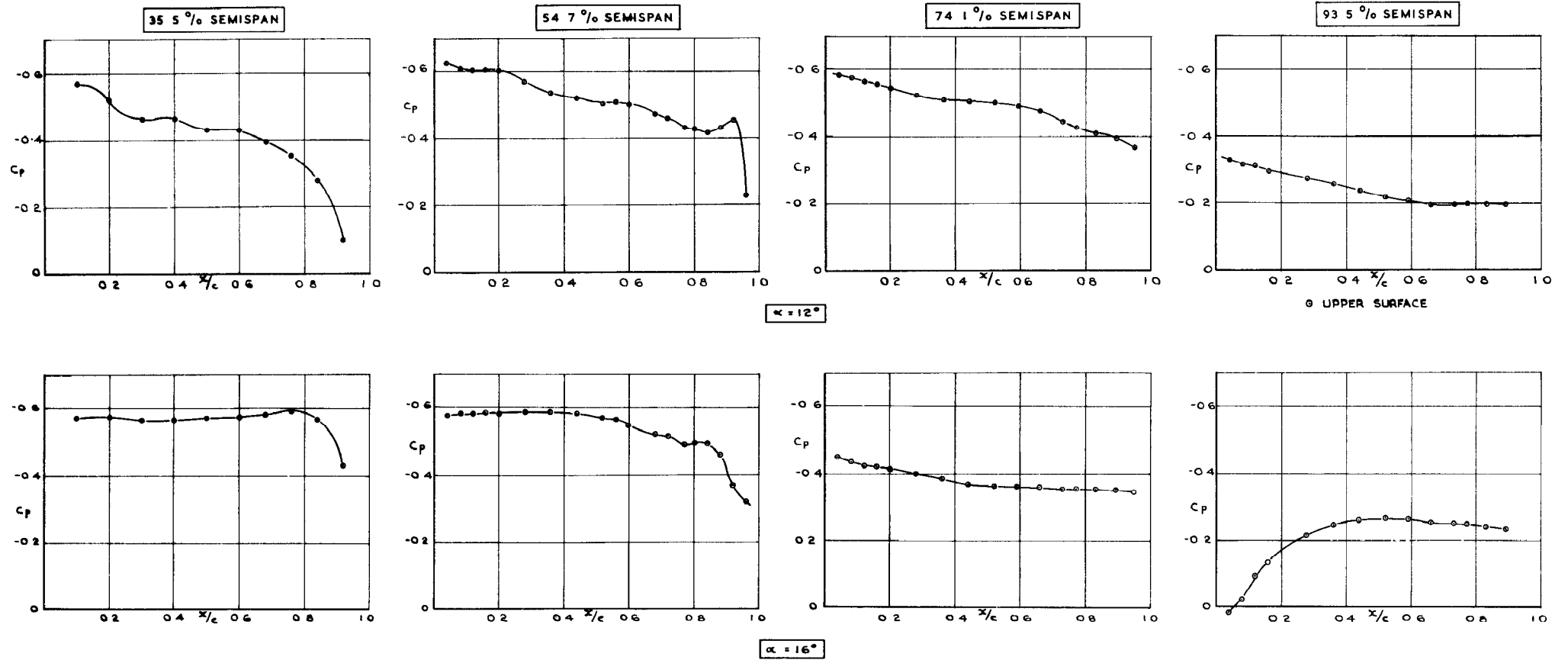


FIG. 23. (a) CHORDWISE PRESSURE DISTRIBUTIONS FOR WING INCIDENCES
 $\alpha = 12, 16$ DEGREES AT $M = 1.42$; $Re, No. = 2.07 \times 10^6$

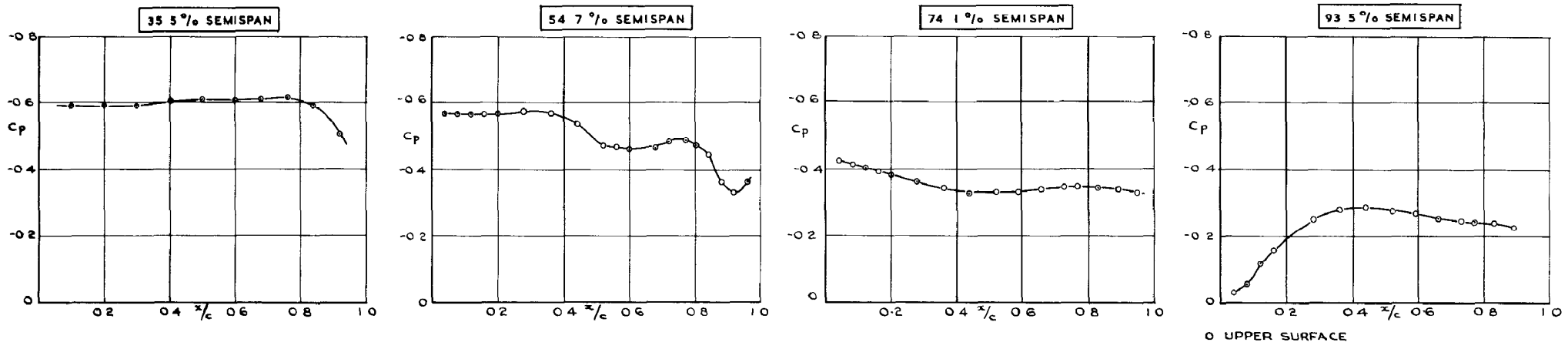


FIG. 23. (b) CHORDWISE PRESSURE DISTRIBUTIONS FOR WING INCIDENCE $\alpha = 18$ DEGREES AT $M = 1.42$; $Re. No. = 2.07 \times 10^6$

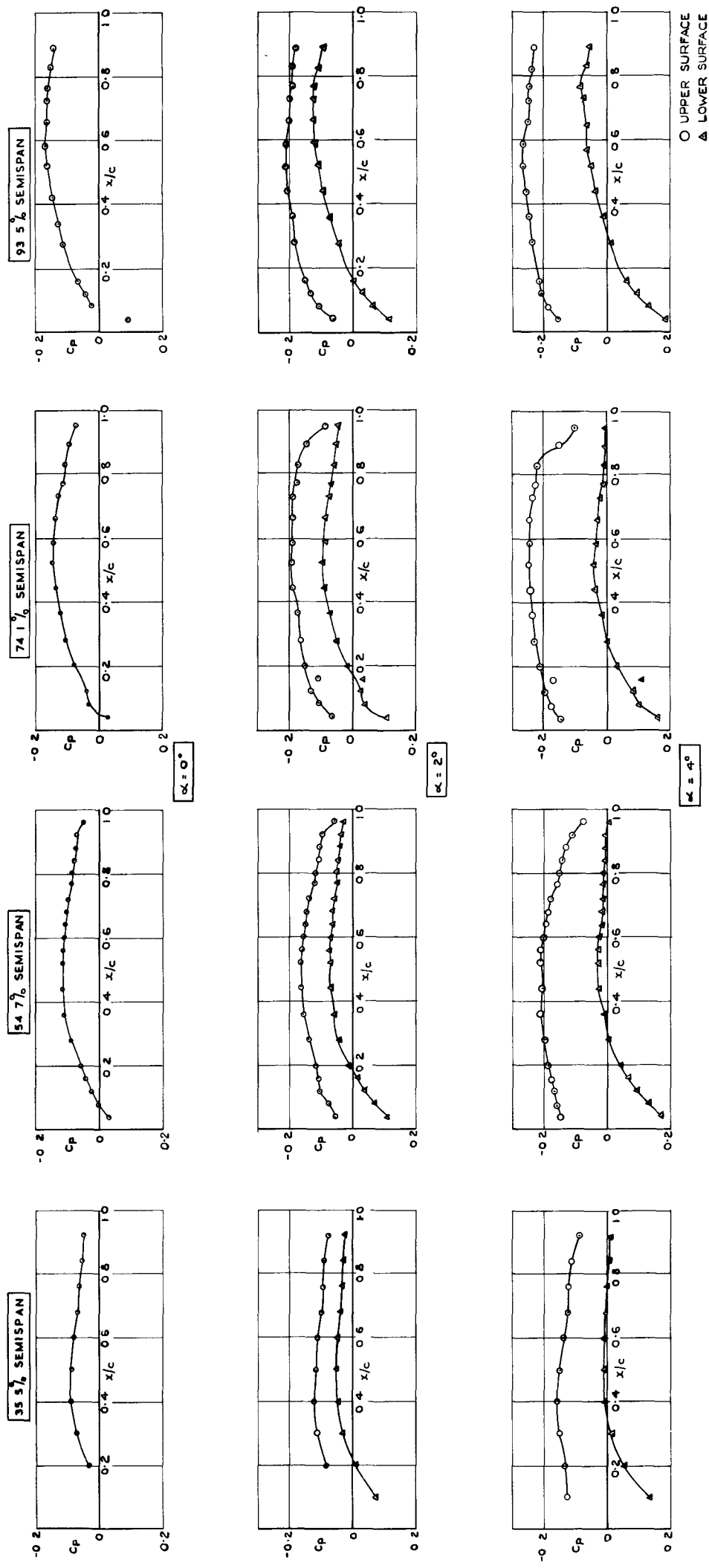


FIG 24. CHORDWISE PRESSURE DISTRIBUTIONS FOR WING INCIDENCES $\alpha = 0, 2, 4$ DEGREES AT $M = 1.82$; RE. No. = 4.15×10^6

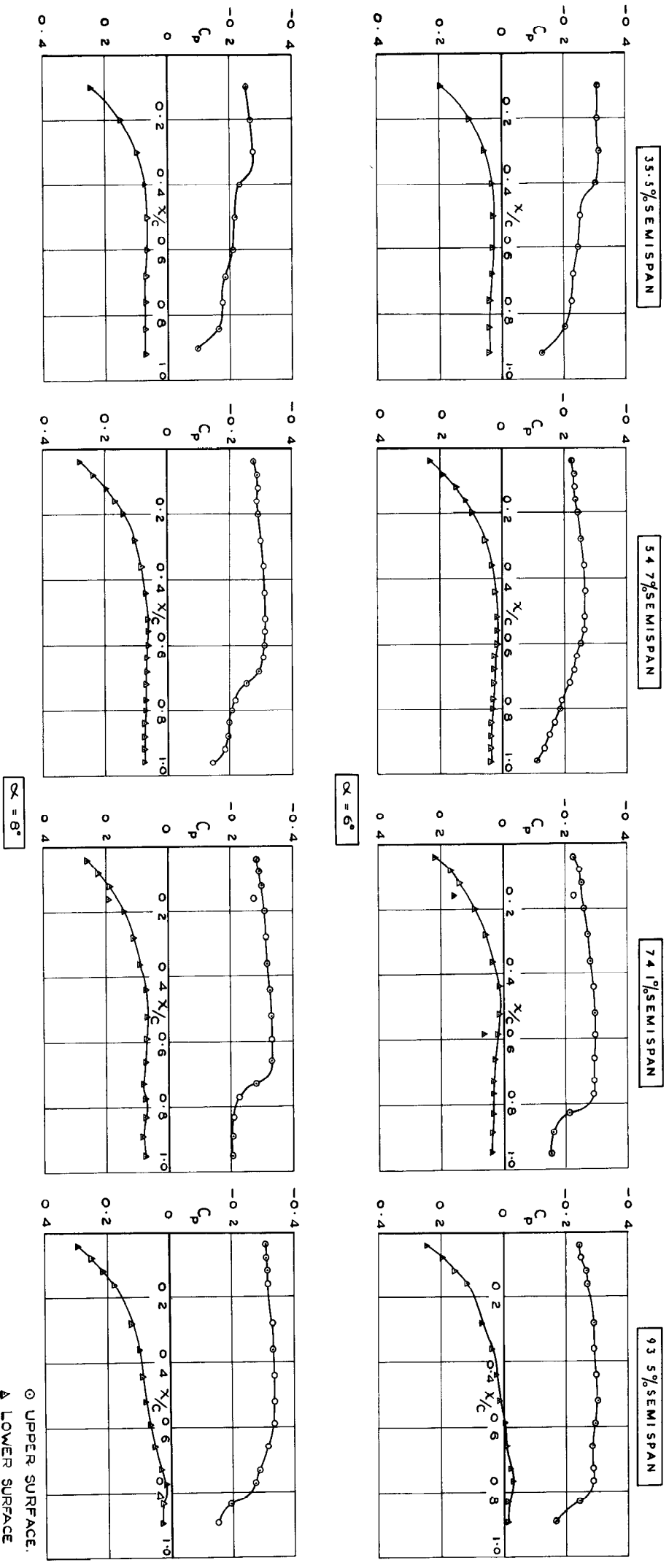
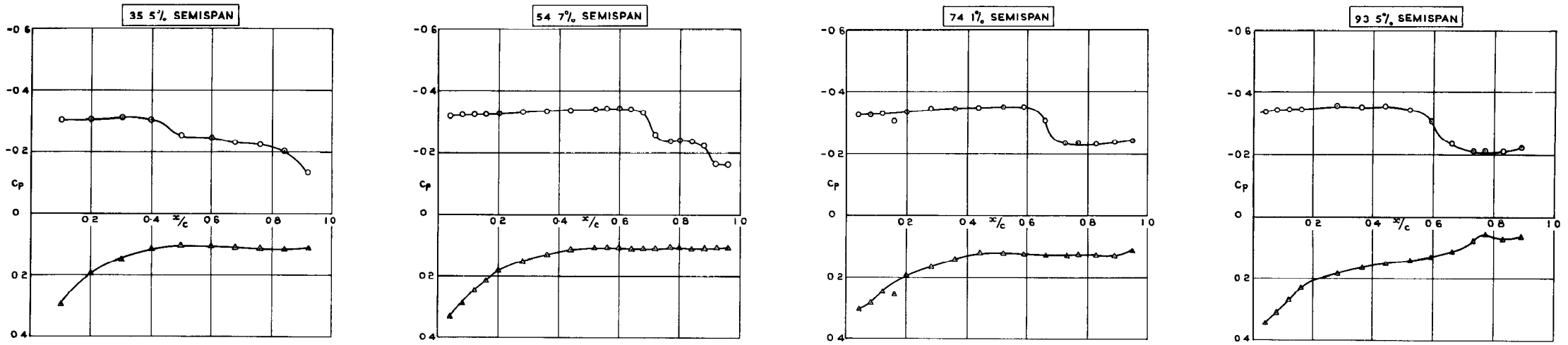
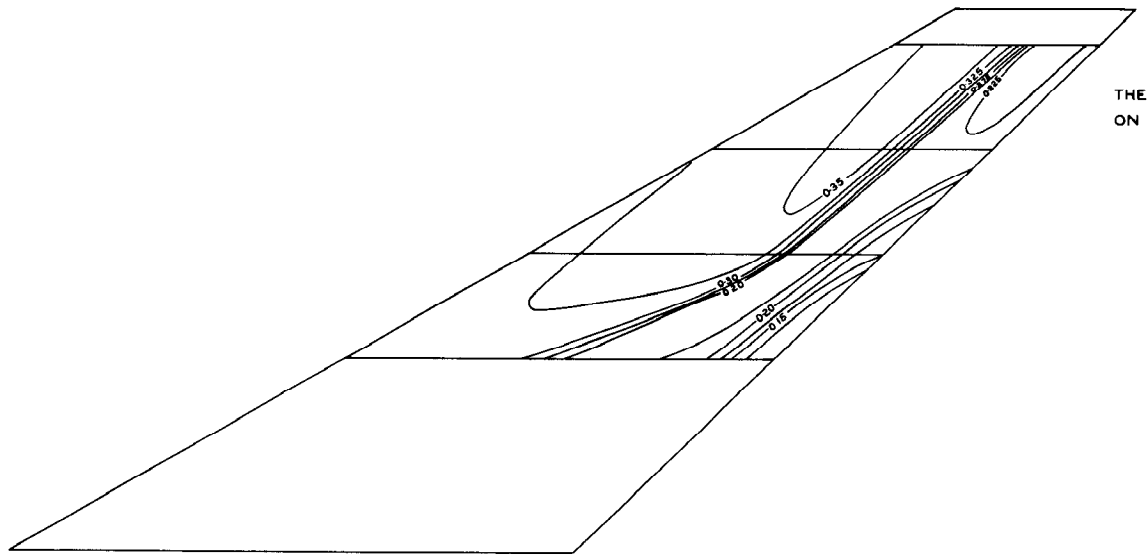


FIG. 25. CHORDWISE PRESSURE DISTRIBUTIONS FOR WING INCIDENCES
 $\alpha = 6, 8$ DEGREES AT $M=1.82$; $RE. NO.=4.15 \times 10^6$



O UPPER SURFACE.
 ▲ LOWER SURFACE.



THE PARAMETER INDICATED
 ON THE ISOBARS IS — C_p

FIG. 26. CHORDWISE PRESSURE DISTRIBUTIONS FOR WING INCIDENCE $\alpha = 10$ DEGREES AT $M=1.82$ AND CORRESPONDING ISOBAR DIAGRAM FOR UPPER SURFACE; $Re.No.=4.15 \times 10^6$

THE ARROWS INDICATE THE SPANWISE POSITIONS OF THE PRESSURE STATIONS

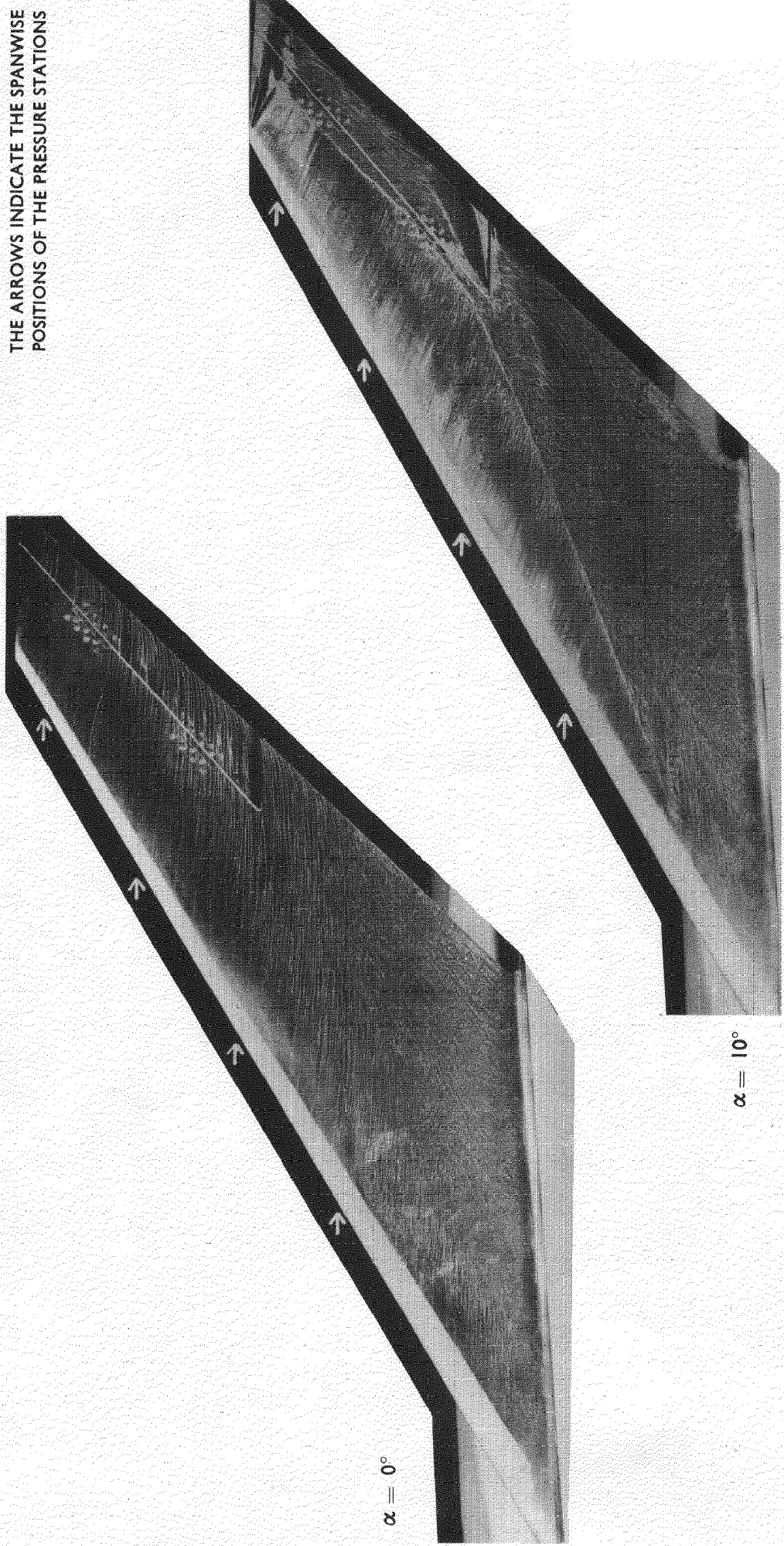


FIG.27. OIL FLOW OBSERVATIONS ON UPPER SURFACE FOR WING INCIDENCES
 $\alpha = 0, 10^\circ$ AT $M = 1.82$; $Re No. = 4.15 \times 10^6$

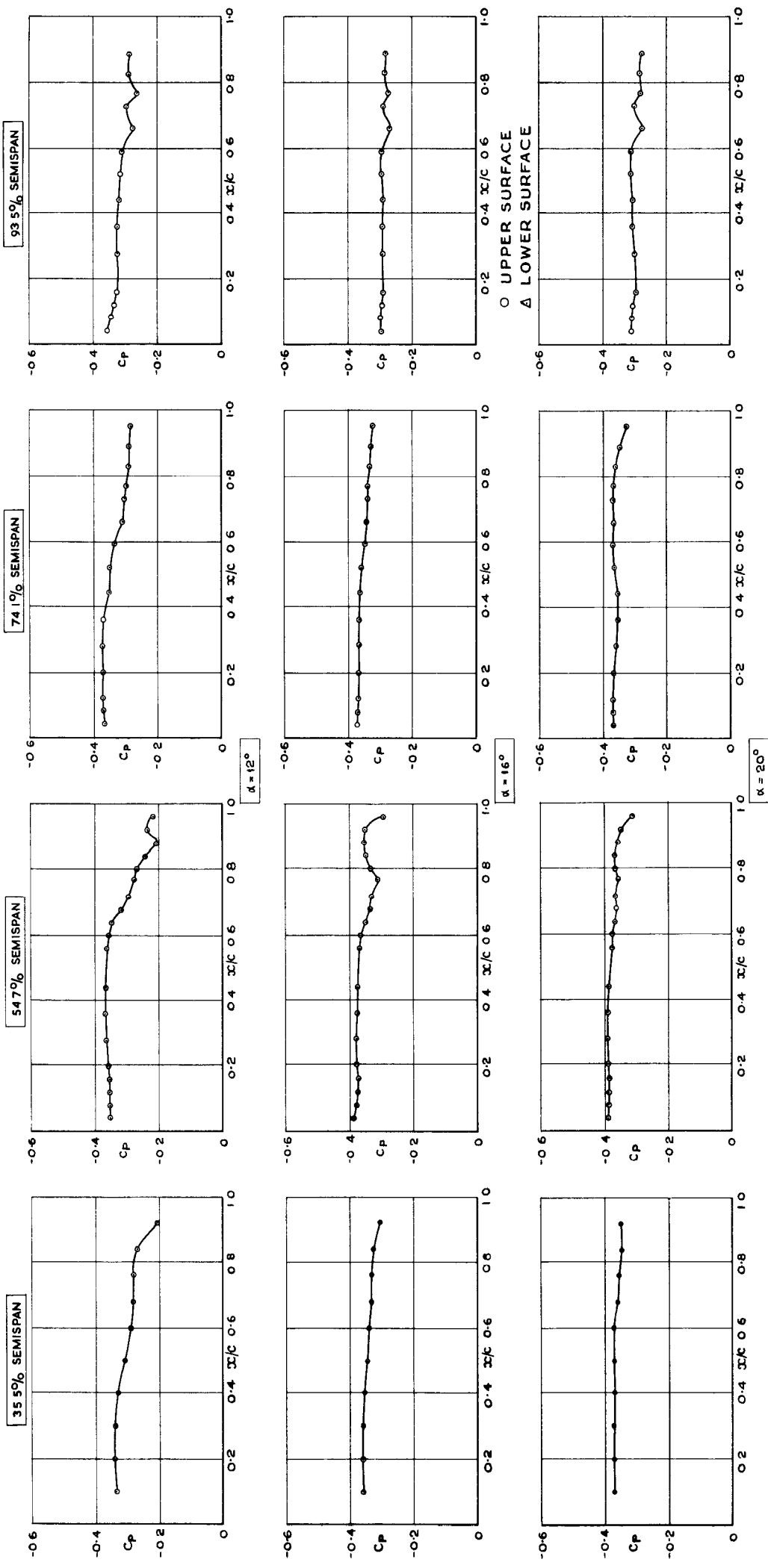


FIG. 28. CHORDWISE PRESSURE DISTRIBUTIONS FOR WING INCIDENCES $\alpha = 12, 16, 20$, DEGREES AT $M=1.82$, $RE. No=2.07 \times 10^6$

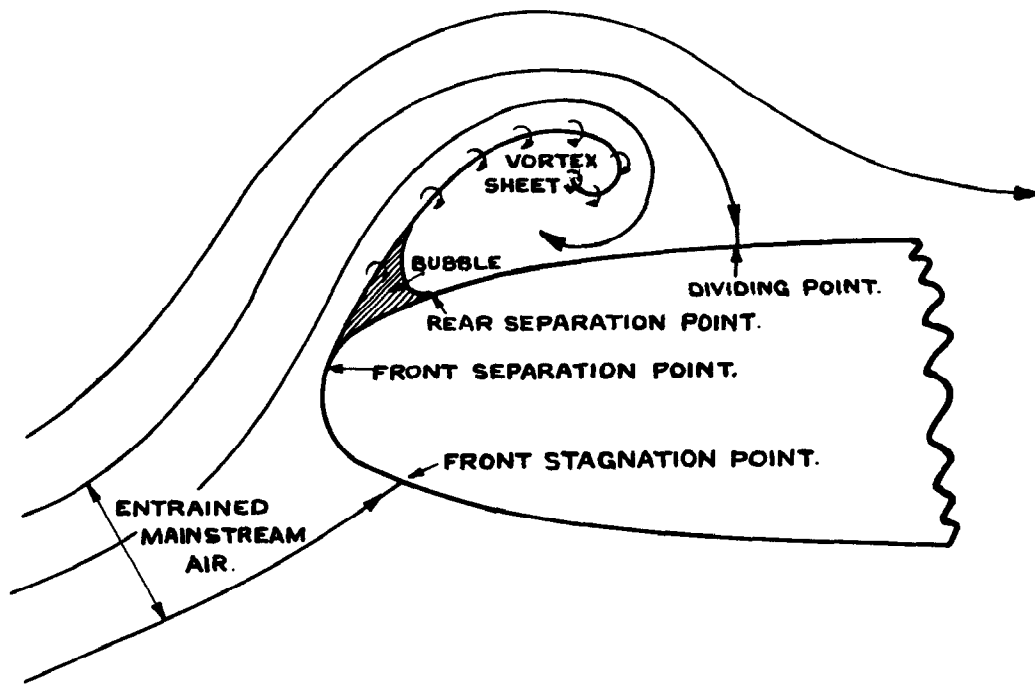


FIG. 29. SKETCH OF PART SPAN VORTEX FLOW FOR A SECTION NORMAL TO THE LEADING EDGE

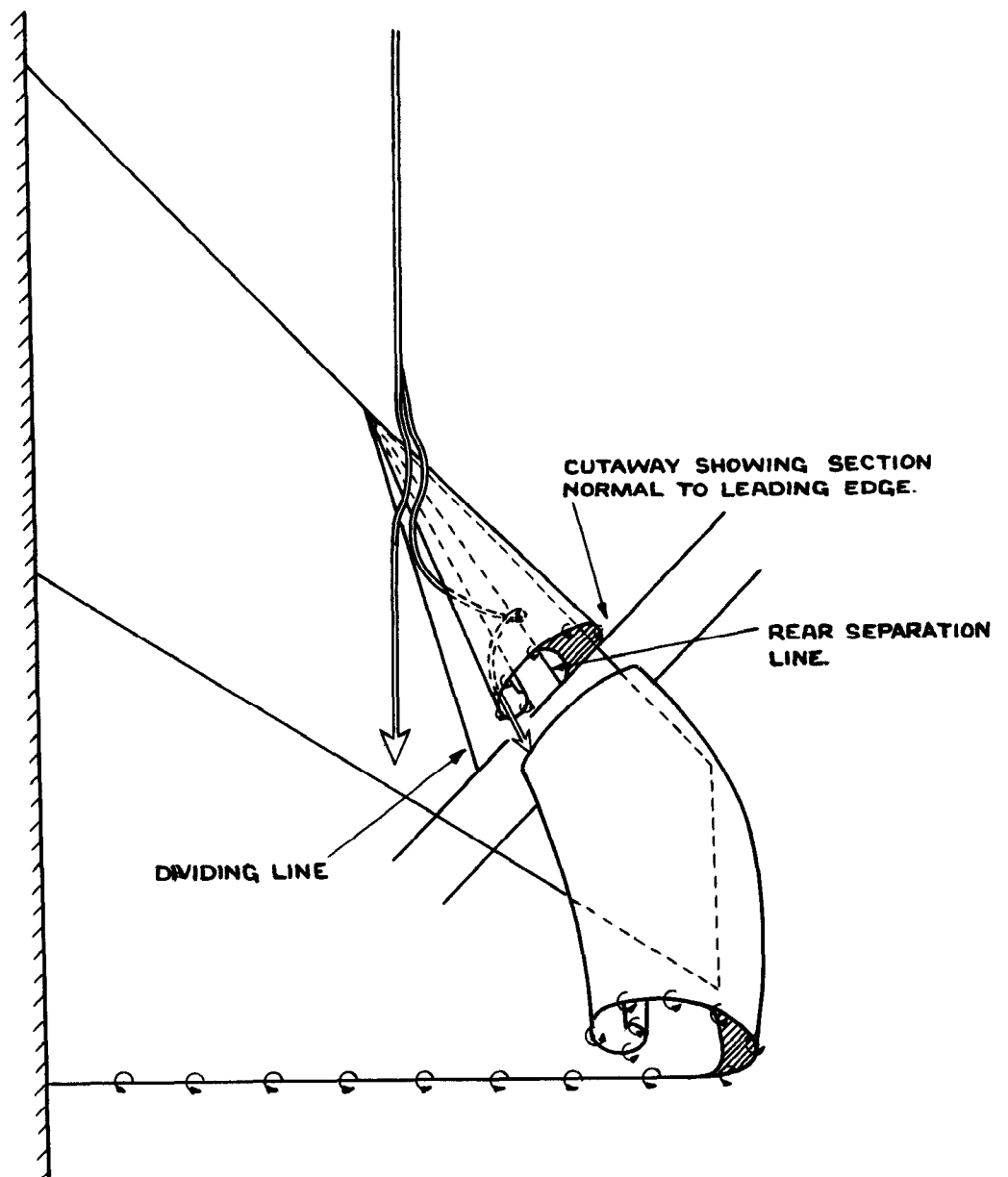


FIG. 30. SKETCH OF FLOW WITH LEADING EDGE SEPARATION & PART SPAN VORTEX

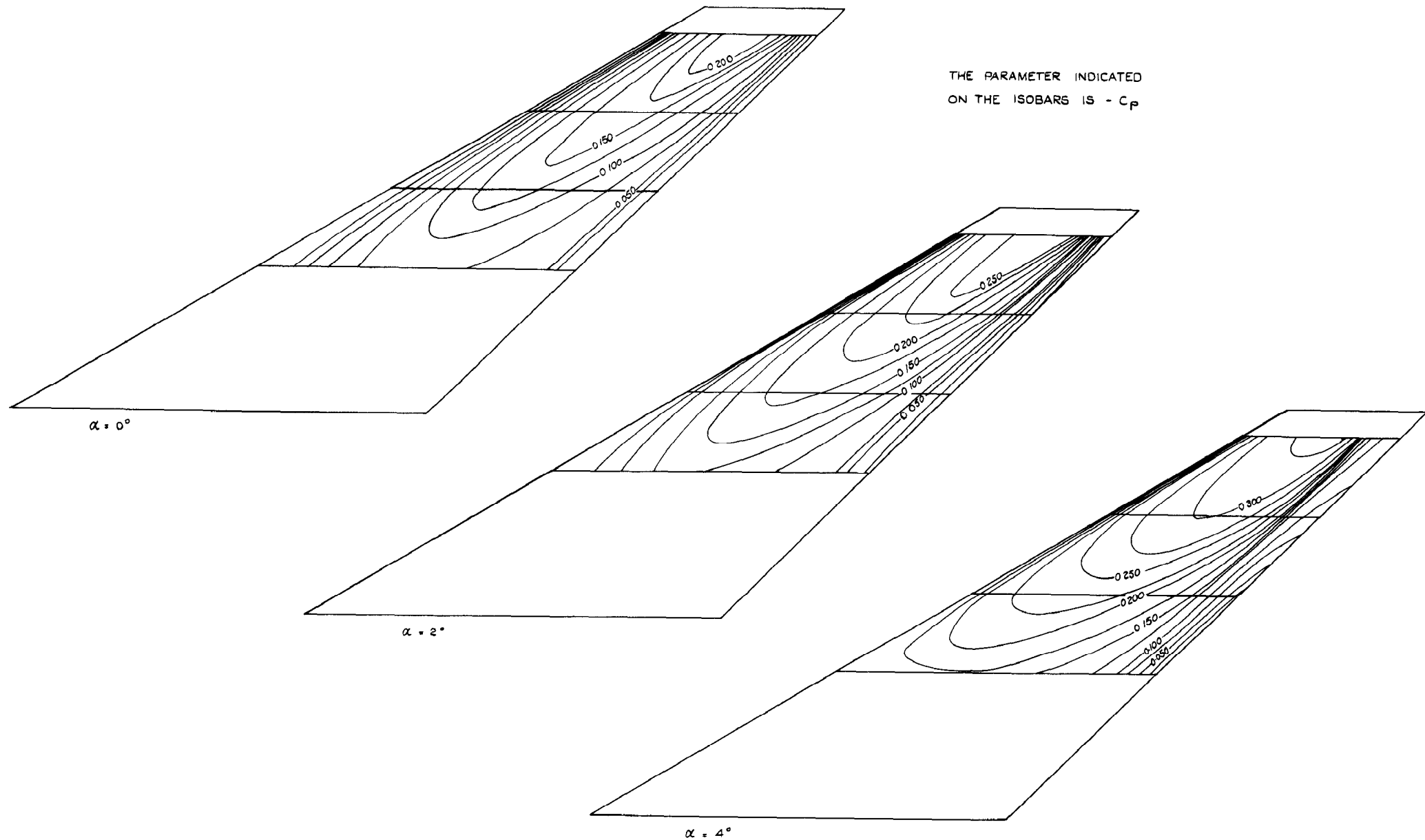


FIG. 31(a) ISOBAR DIAGRAMS FOR UPPER SURFACE FOR INCIDENCES
 $\alpha = 0, 2, 4$ DEGREES AT $M = 1.61$; $Re. No. = 4.15 \times 10^6$

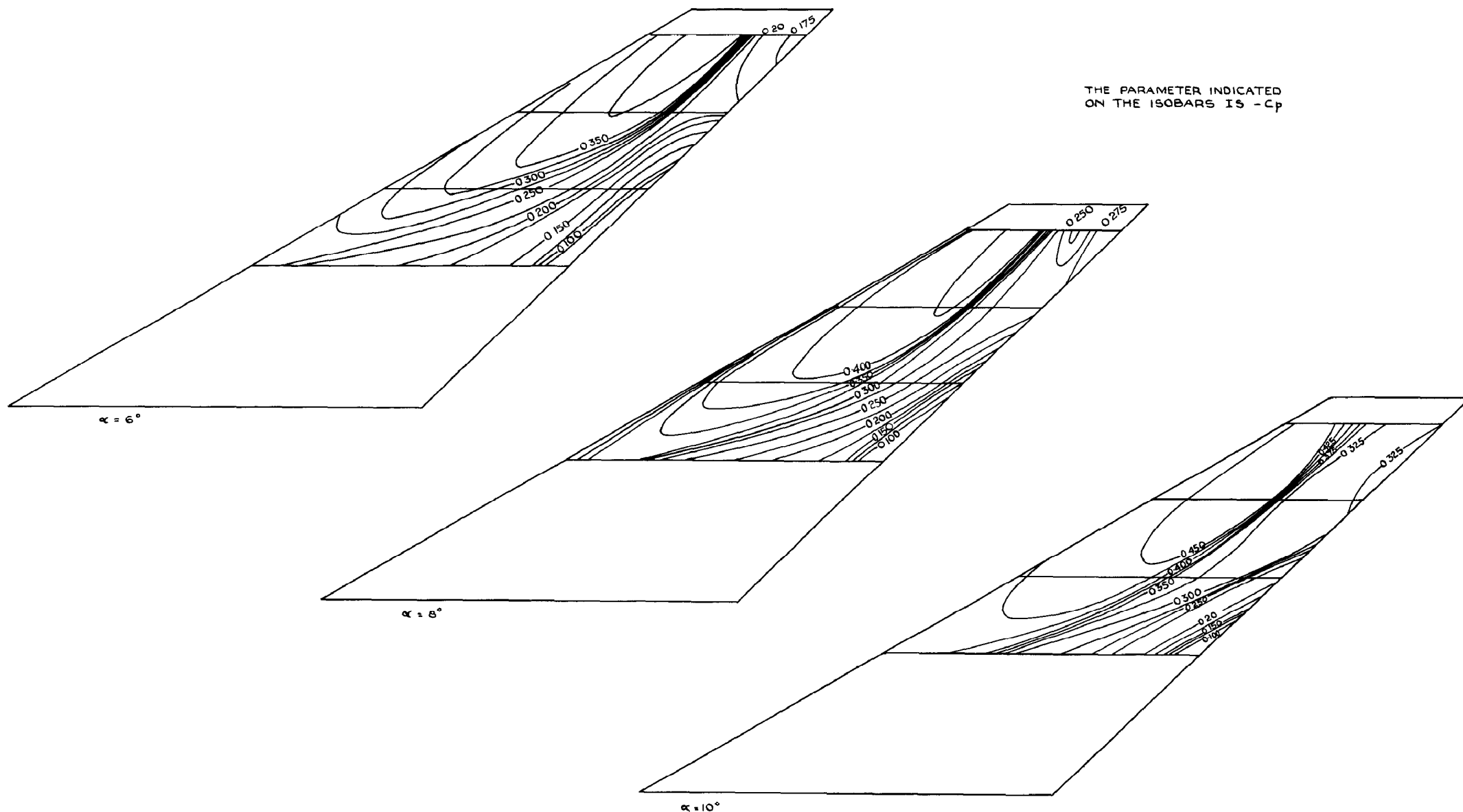


FIG. 31 (b). ISOBAR DIAGRAMS FOR UPPER SURFACE FOR INCIDENCES $\alpha = 6, 8, 10$ DEGREES AT $M = 1.61$; $Re. No. = 4.15 \times 10^6$

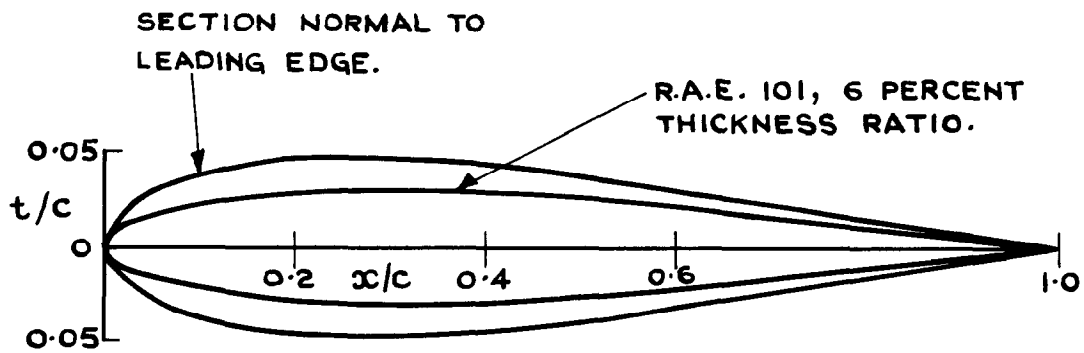


FIG. 32. COMPARISON OF SECTION NORMAL TO LEADING EDGE WITH STREAMWISE SECTION 6 PERCENT THICK R.A.E. 101

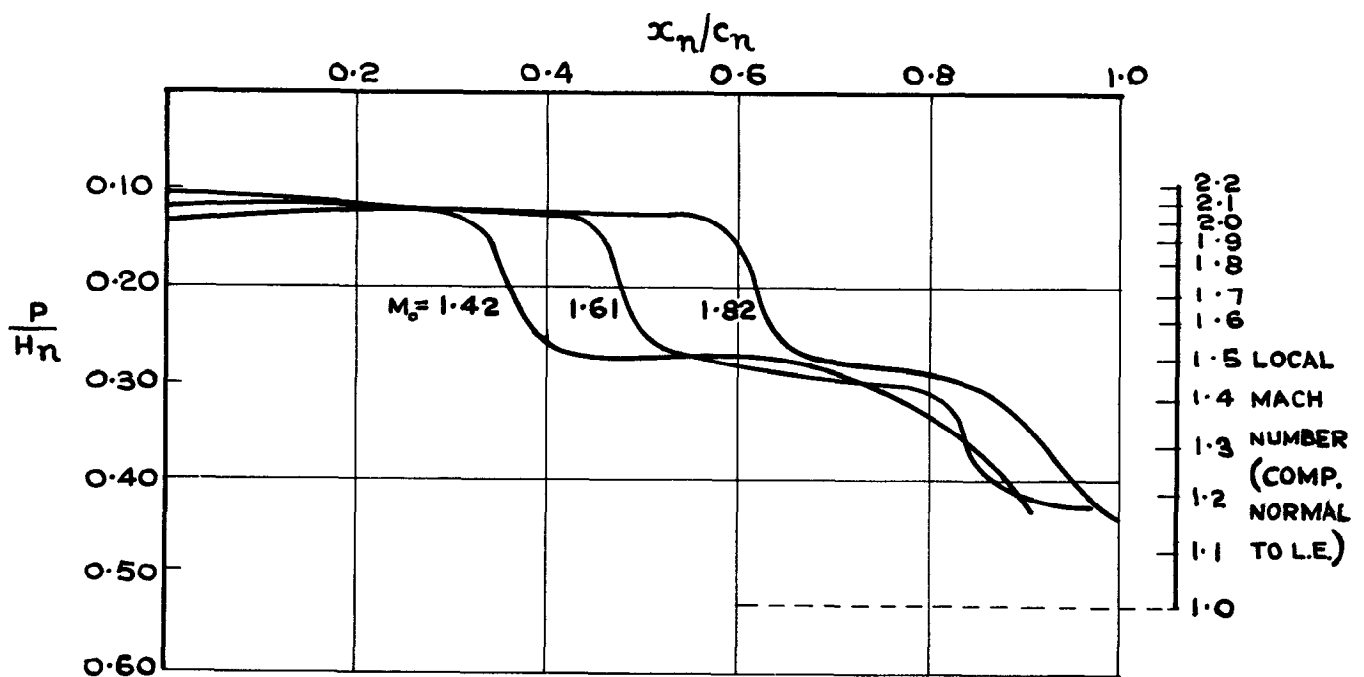


FIG. 33. PRESSURE DISTRIBUTIONS ON UPPER SURFACE TAKEN NORMAL TO THE LEADING EDGE FOR THREE SUPERSONIC SPEEDS AT WING INCIDENCE $\alpha = 10$ DEGREES

© *Crown Copyright 1960*

Published by
HER MAJESTY'S STATIONERY OFFICE

To be purchased from
York House, Kingsway, London w.c.2
423 Oxford Street, London w.1
13A Castle Street, Edinburgh 2
109 St. Mary Street, Cardiff
39 King Street, Manchester 2
Tower Lane, Bristol 1
2 Edmund Street, Birmingham 3
80 Chichester Street, Belfast
or through any bookseller

Printed in England